The Messinian salinity crisis in Cyprus: a further step toward a new stratigraphic framework for Eastern Mediterranean

(Article begins on next page)

UNIVERSITÀ DEGLI STUDI DI TORINO

This is an author version of the contribution published on:
Questa è la versione dell'autore dell'opera:

The Messinian salinity crisis in Cyprus: a further step towards a new stratigraphic framework for Eastern Mediterranean

Vinicio Manzi,*,† Stefano Lugli,‡ Marco Roveri,*,† Francesco Dela Pierre,§
Rocco Gennari,*,† Francesca Lozar,§ Marcello Natalicchio,§ B. Charlotte Schreiber,¶
Marco Taviani**,†† and Elena Turco*,†

*Parma University, Parma, Italy
†ALP, Alpine Laboratory of Palaeomagnetism, Peveragno, CN, Italy
‡Modena and Reggio Emilia University, Modena, Italy
§Torino University, Torino, Italy
¶University of Washington, Seattle, WA, USA
**ISMAR-CNR Bologna, Bologna, Italy
††Woods Hole Oceanographic Institution, Woods Hole, MA, USA

The definitive version is available at:
La versione definitiva è disponibile alla URL:
http://onlinelibrary.wiley.com/doi/10.1111/bre.12107/full

TheMessinian salinity crisis in Cyprus: a further step towards a newstratigraphic framework for EasternMediterranean

Vinicio Manzi,*,† Stefano Lugli,‡ Marco Roveri,*,† Francesco Dela Pierre,§
Rocco Gennari,*,† Francesca Lozar,§ Marcello Natalicchio,§ B. Charlotte Schreiber,¶
Marco Taviani**,†† and Elena Turco*,†

*Parma University, Parma, Italy
†ALP, Alpine Laboratory of Palaeomagnetism, Peveragno, CN, Italy
‡Modena and Reggio Emilia University, Modena, Italy
§Torino University, Torino, Italy
¶University of Washington, Seattle, WA, USA
**ISMAR-CNR Bologna, Bologna, Italy
††Woods Hole Oceanographic Institution, Woods Hole, MA, USA

ABSTRACT

A revised stratigraphic framework for the Messinian succession of Cyprus is proposed demonstrating that the three-stage model for the Messinian salinity crisis recently established for the Western Mediterranean also applies to the Eastern Mediterranean, at least for its marginal basins. This analysis is based on a multidisciplinary study of the Messinian evaporites and associated deposits exposed in the Polemi, Pissouri, Maroni/Psematismenos and Mesaoria basins. Here, we document for the first time that the base of the unit usually referred to the 'Lower Evaporites' in Cyprus does not actually correspond to the onset of the Messinian salinity crisis. The basal surface of this unit rather corresponds to a regional-scale unconformity, locally associated with an angular discordance, and is related to the erosion and resedimentation of primary evaporites deposited during the first stage of the Messinian salinity crisis. This evidence suggests that the 'Lower Evaporites' of the southern basins of Cyprus actually belong to the second stage of the Messinian salinity crisis; they can be thus ascribed to the Resedimented Lower Gypsum unit that was deposited between 5.6 and 5.5 Ma and is possibly coeval to the halite deposited in the northern Mesaoria basin. Primary, in situ evaporites of the first stage of the Messinian salinity crisis were not preserved in Cyprus basins. Conversely, shallow-water primary evaporites deposited during the third stage of the Messinian salinity crisis are well preserved; these deposits can be regarded as the equivalent of the Upper Gypsum of Sicily. Our study documents that the Messinian stratigraphy shows many similarities between the Western and Eastern Mediterranean marginal basins, implying a common and likely coeval development of the Messinian salinity crisis. This could be reflected also in intermediate and deep-water basins; we infer that the Lower Evaporites seismic unit in the deep Eastern Mediterranean basins could well be mainly composed of clastic evaporites and that its base could correspond to the Messinian erosional surface.

INTRODUCTION

Dating the onset of the Messinian salinity crisis (MSC) has been the main target of numerous integrated (cyclo-, bio-, magneto-) stratigraphic studies carried out in the Mediterranean during the past few years (Krijgsman et al., 1999; Hilgen & Krijgsman, 1999; Bellanca et al., 2001; Sierro et al., 2001; Blanc-Valleron et al., 2002; Krijgsman et al., 2002; Krijgsman et al., 2004; Kouwenhoven et al., 2006; Rouchy & Caruso, 2006 and reference therein; Manzi et al., 2007; Gennari et al., 2013; Manzi et al., 2013 and references therein). These studies were mainly undertaken to facilitate the reconstruction of the environmental changes that occurred at the onset of the salinity crisis when the Mediterranean basin, or parts of it, was turned into a giant salina. Following years of debate about the synchronous vs. diachronous character of the MSC onset (Rouchy & Caruso, 2006; Roveri et al., 2014a), a consensus was reached by a large number of scientists involved in Messinian research (CIESM, 2008) on a chronostratigraphic frame work conditions throughout the Mediterranean.

An important issue exists regarding the criteria that can be used in the definition of the onset of the Messinian salinity crisis. Recent advancements in the sedimentology and stratigraphy of the Lower Evaporites deposits (CIESM, 2008; Roveri et al., 2008a; Lugli et al., 2010; Dela Pierre et al., 2011, 2012; Manzi et al., 2011; Gennari et al., 2013; Manzi et al., 2013) revealed that the onset of the Messinian salinity crisis is commonly improperly positioned both in shallow and deep settings.

In shallower settings, the inappropriate definition of the onset of the MSC is commonly related to the presence of incomplete Primary Lower Gypsum (PLG) successions that prevent a precise tuning of the first local gypsum bed. As recently demonstrated (De Lange & Krijgsman, 2010; Lugli et al., 2010; Dela Pierre et al., 2011; Manzi et al., 2013), the gypsum beds of the PLG unit are laterally transitional to carbonate or shale deposits. When this occurs, the first local gypsum bed does not coincide with the onset of the MSC but could be younger by 1 (Perales

section, Manzi et al., 2013), 2 (Legnagnone section; Gennari et al., 2013), 3 (Pollenzo section; Dela Pierre et al., 2011, 2012) or even 6 precessional cycles (Govone section; Bernardi, 2013).

In deeper settings, the definition of the onset of the MSC could be even more complicated because: (i) PLG deposits never accumulated there and their time equivalents deposits are commonly represented by evaporitefree units deposited in a restricted environment (Manzi et al., 2007, 2011; Roveri et al., 2008a,b); (ii) the evaporate units commonly include large amount of clastics; and (iii) hiatuses of variable duration are associated to the Messinian erosional surface (MES) lying at the base of the Resedimented Lower Gypsum unit (RLG; Roveri et al., 2008a,b).

In all those cases where, based on integrated (bio-magneto- cyclo) stratigraphic analyses, a latest early Messinian, pre-MSC, age is defined but the correct tuning of the PLG unit is not possible, the MSC onset is approximated by one or more of the following proxies (see more detailed information in Manzi et al., 2007, 2011): (i) the base of the PLG time-equivalent dolomite-rich unit; (ii) the Last Occurrence (LO) of foraminifera either planktonic or benthic (Manzi et al., 2007; Lozar et al., 2010; Dela Pierre et al., 2011; Gennari et al., 2013; Manzi et al., 2013); (iii) the peak of abundance of Sphenolithus abies (Manzi et al., 2007; Lozar et al., 2010); (iv) the presence of high-salinity tolerant pteropod assemblages (Manzi et al., 2007); (v) the recognition of the base of the reversal Gilbert chron (the MSC onset is three precession cycles above it; Manzi et al., 2013); (vi) the $d_{18}O$ shift toward high positive values (Bellanca et al., 2001; Manzi et al., 2011); and (vii) the occurrence of peculiar molecular indicators (gammacerane; <0.2 pristane/phytane ratio; <1 nalkanes odd/even predominance; Manzi et al., 2007).

These observations were mainly derived from the Messinian successions cropping out in the western/central Mediterranean (Spain, Sicily, Apennines), whereas the eastern Mediterranean was far less taken into consideration.

In the eastern Mediterranean on-land successions, the studies carried out over the past few years focused on the pre-evaporitic successions (Krijgsman et al., 2002; Kouwenhoven et al., 2006; Morigi et al., 2007; Orszag- Sperber et al., 2009). The main aim of these studies was the correlation of the onset of the MSC with the Western Mediterranean. Actually, these studies provide a high-resolution stratigraphic framework that is limited to the pre-MSC succession due to the lack of sufficiently detailed sedimentologic and stratigraphic information on the overlying evaporites. Up to now, the comparison between the eastern and western MSC records has been essentially based on the seismic aspects of the deep evaporites. The typical threefold succession (Lower Evaporites, Salt, Upper Evaporites) characterizing the Western Mediterranean is not present in the Eastern Mediterranean where the MSC is largely recorded by a single salt-bearing seismic unit (Lofi et al., 2011 and references therein). In any event, more recently, an attempt of correlating western and eastern deep Mediterranean Messinian seismic units has been suggested, based on Sr isotope and high-resolution seismic data (Roveri et al., 2014b).

Thus, a question still remains unanswered: was the onset of the MSC synchronous in the eastern and western Mediterranean or not?

In this study, we present new results derived from a multidisciplinary approach, integrating physical stratigraphy, facies analysis, sedimentology, petrography and biostratigraphy and magnetostratigraphy of the upper portion of the Pakhna Formation (Bagnall, 1960; Gass, 1960; Pantazis, 1967; Robertson et al., 1995) and the overlying evaporites of the Kalavasos Formation (Bagnall, 1960; Gass, 1960; Pantazis, 1967; Robertson et al., 1995) in several basins of Cyprus. We focus particularly on the different evaporite facies and stratigraphic architecture and on the timing of their onset in Cyprus. The main aim of this study was to test the applicability of the stratigraphic framework established for the western Mediterranean and to shed new light on the relationships between the onshore vs. offshore record of the Messinian salinity crisis in the eastern Mediterranean.

CHRONOSTRATIGRAPHIC FRAMEWORKOFMESSINIAN EVENTS

The chronostratigraphic framework proposed for the Messinian salinity crisis (Fig. 1; CIESM, 2008; Roveri et al., 2008a,b, 2014a), derives from a thorough review and analyses of the sedimentary facies, petrography and stratigraphy of Messinian evaporites (Roveri et al., 2001, 2008a,b, 2014a,b; Roveri et al., 2003; Manzi et al., 2005, 2009, 2012; Lugli et al., 2010; Omodeo-Sal_e et al., 2012) and of their time-equivalent deposits (Manzi et al., 2007, 2011, 2013; Omodeo-Sal_e et al., 2012); it considers three depositional stages (Fig. 1). During stage 1 (5.97− 5.60 Ma; Krijgsman et al., 1999; Manzi et al., 2013), the Primary Lower Gypsum (PLG; Roveri et al., 2008a), mainly consisting of sulphate bottom-grown evaporites, accumulated exclusively in shallow-water settings (i.e. <200 m of depth), whereas deeper-water settings experienced euxinic shale and carbonate deposition (De Lange & Krijgsman, 2010). Later, during stage 2 (5.60− 5.53 Ma), shallow-water peri-Mediterranean areas were exposed to subaerial erosion and evaporite deposition migrated to the deeper parts of the basin (Roveri et al., 2014a). The evaporites deposited during this stage consist of both clastic (gypsum-carbonate deposits derived from the resedimentation of the PLG) and primary deposits (halite with a minor sulphate contribution), grouped into the Resedimented Lower Gypsum unit (RLG; Roveri et al., 2008a). Finally, during stage 3 (5.53−5.33 Ma; Hilgen et al., 2007; Manzi et al., 2009), a new evaporite unit was deposited in both shallow (primary shallow water, mostly bottom-grown facies) and deep settings (clastic and cumulate gypsum).

GEOLOGICAL AND GEODYNAMIC SETTING OF CYPRUS

Cyprus Island is located in a complex tectonic area characterized by the interaction between the African, Arabia and Eurasian plates (Fig. 2a). The Cyprus Arc (Fig. 2b) represents the present-day boundary between the Eurasian and African plates. From this point of view, it represents the easternmost portion of the Mediterranean Ridge (Fig. 2a; Chaumillon et al., 1996; Mascle & Chaumillon, 1998; Huguen et al., 2001; Le Pichon et al., 2002; Ten Veen et al.,

2004), a complex structure extending from the Ionian Islands of western Greece to Turkey in an east–west direction (Fig. 2) that originated from the northward subduction of the Ionian oceanic crust, a remnant of the Tethys Ocean, under the European plate (Robertson, 1976; 1998; Huguen et al., 2001). In the Ionian basin, the subduction is still active, whereas moving eastward the geodynamic setting is complicated by the ongoing collision between the Eurasian and the African plates. In the easternmost portion of the Mediterranean, the presence of the Eratosthenes microplate, a small block of African continental crust (Robertson, 1998) caused the emersion of the accretionary prism and the birth of the Island of Cyprus. According to recent studies (Kinnaird et al., 2011; Kinnaird & Robertson, 2013), the structure of Cyprus derived by the stacking of three tectonic slices that from the north passing to the south are as follows: the Kyrenia Ridge, the Troodos massif (an ophiolite unit that represents the remnant of an original oceanic crust) and the Mamonia complex (Fig. 2).

Recent tectonic reconstructions based on a structural analysis of faults and fractures recognized in Cyprus (Kinnaird & Robertson, 2013; McCay & Robertson, 2013) suggest that the Cyprus area was affected by a complex tectonic evolution during the Neogene including: (i) an early Miocene compressional phase; (ii) an extensional phase during the late Miocene and Early Pliocene times and finally; and (iii) a compressional/transpressional phase up to recent times. Apart from the information on the changes in the main stress vectors, the history of Cyprus since the late Mesozoic can be also deduced by the observation of change in facies distribution and depositional settings in the circum- Troodos sedimentary succession that is schematically reported in Fig. 3 (Robertson et al., 1995). The first clear evidence of the formation of significant landmass with a permanent subaerial drainage pattern dates to the Pliocene (Eaton & Robertson, 1993; Robertson et al., 1995; Stow et al., 1995). According to the most recent hypothesis (Kinnaird et al., 2011; Kinnaird & Robertson, 2013), the Troodos uplift began in late Pliocene (<2.58 Ma). However, this could be considered only the final part of a much longer history of erosion and deposition of the Troodos sedimentary cover; first, late Mesozoic-Miocene pelagic units were eroded, then the definitive uplift and erosion of the Troodos oceanic crust slice was recorded by the late Pliocene progradation of ophiolite-derived fan-deltas into the Mesaoria basin. For the aim of this article, it is more interesting focusing on the depositional history that preceded the Messinian salinity crisis. The progressive shallowing upward trend of the early Cenozoic Lefkara Formation (Fig. 3; Bagnall, 1960; Gass, 1960; Pantazis, 1967; Payne & Robertson, 1995; Robertson et al., 1995) and the widespread distribution of Miocene carbonate reefs and carbonate platforms (Robertson et al., 1995; Follows, 1992; Follows et al., 1996) now outcropping along the northern and southern margins of the Troodos massif, suggest an earlier uplift of the Troodos area, probably since the Oligocene. The presence in the Koronia member of late Tortonian-early Messinian reefs (Follows et al., 1996), suggests that the Troodos area was already at very shallow water depth at that time. Furthermore Troodos- derived pebbles are reported in the conglomerates of the Lago-Mare unit of the Pissouri basins (Rouchy et al., 2001) suggesting that emersion of the Troodos massif could have occurred, at least partially, since the latest Messinian.

Due to its present-day elevated position, Cyprus permits detailed study that leads to a better comprehension of the geology of the Eastern Mediterranean area and to fully exploit the large amount of offshore data acquired in the last decades (Robertson et al., 1995; Bridge et al., 2005; Calon et al., 2005; Aksu et al., 2008; Maillard et al., 2010). The Cyprus Arc subdivides the Eastern Mediterranean in a northern and a southern region, characterized by different geological settings and by a different record of the Messinian salinity crisis. The northern region is in turn segmented into three main arched basins elongated in a E-W direction (Fig. 2b).

The northern basin, corresponding to the Cilicia basin, is completely submerged and is known from seismic data (Bridge et al., 2005; Calon et al., 2005; Aksu et al., 2008). This basin is bounded to the south by a E-W trending structural high corresponding to the Kyrenia Range, a mountain ridge exposed in the northernmost part of Cyprus, characterized by Mesozoic carbonate terrains at its core (McCay et al., 2013).

The central basin includes an onshore portion in the Cyprus Island known as the Mesaoria basin (McCallum & Robertson, 1995) that continues offshore to the west into the northern Antalya basin and to the east into the Larnaca-Latakia (Maillard et al., 2010) and Iskenderun basins (Calon et al., 2005), in Turkey. Messinian deposits crop out only in the northern and southern flanks of the basin, but the presence of a thick Messinian halite unit buried below the Mesaoria plain, has been documented by seismic profiles and boreholes (Gass, 1960; Robertson et al., 1995; Maillard et al., 2010). Seismic data suggest the presence of salt deposits offshore as well (Maillard et al., 2010). The central basin is bounded to the south by a structural high culminating with the Troodos Massif.

Finally, the southern basin is articulated in minor subbasins onshore (Polemi, Pissouri and Psematismenos/Maroni basins) and offshore (Tartus basin and Intermediate basin; Maillard et al., 2010).

All these basins are characterized by a relatively thin (commonly <500 m-thick) Messinian succession including sulphate and also halite, as suggested by the presence of small diapirs imaged by seismic both in the Latakia and Tartus basins (see Maillard et al., 2010 for further information). Conversely the southern region, corresponding to the Levant basin, shows a very thick Messinian evaporate unit (between 1 and 2 km) mainly consisting of halite (Hübscher et al., 2007; Cartwright & Jackson, 2008; Maillard et al., 2010) with minor clastic intercalations that is still relatively undeformed (Bertoni & Cartwright, 2006, 2007; Lofi et al., 2011; Gvirtzman et al., 2013).

STRATIGRAPHIC SETTING OF CYPRUS

According to Robertson et al. (1995) the sedimentary succession of Cyprus Island can be summarized as follows (Figs 2 and 3).

Pre-Messinian

The first sedimentary deposits, laying directly on a magmatic basement, are represented by umbers and radiolarites of the Perapedhi Formation followed by the volcaniclastic Kannaviou Formation (Bagnall, 1960).Starting from the Maastrichtian the succession continues with the Lefkara Formation (Robertson et al., 1995) previously known as Lapithos group (Bagnall, 1960; Gass, 1960) or as Lefkara Group (Pantazis, 1967), a unit consisting of deep water pelagic marls and carbonate deposited over a prolonged time interval (Late Cretaceous − Oligo-cene; Eaton & Robertson, 1993). This phase of monotonous sedimentation was interrupted by the deposition of the Pakhna Formation (Bagnall, 1960; Gass, 1960; Pantazis, 1967) (Burdigalian/Langhian − lower Messinian; Eaton & Robertson, 1993) that records a phase during which several small, interconnected basins developed, due to the ongoing tectonics related to the collision of the African and European plates.

On top of the intrabasinal highs the pelagic sedimentation was progressively replaced by the formation of reefal and bioclastic deposits related to small carbonate platforms and shoals. Two main carbonate bodies, corresponding, respectively, to the lower Miocene Terra member and the Tortonian/Messinian Koronia member, have been recognized and are described in papers by Pantazis (1967), Bagnall (1960), Gass (1960) and Robertson et al. (1995). According to Follows et al. (1996) the areal and facies distribution of these reefs reflect those of the main structural lineaments active during Miocene time. Interestingly the late Tortonian-early Messinian reef units (Koronia member) are bounded to the south and to the north by the Troodos massif, thus suggesting that this zone was at a water depth within the photic zone at that time. This is in agreement also with the evidence of coeval early and late Miocene submarine mass wasting deposits occurring on both the northern and southern flanks of the Troodos massif that have been related to seismic events punctuating its uplift history (Lord et al., 2009).

Pre-MSCMessinian deposits

Lower Messinian deposits are included in the upper portion of the Pakhna Formation. This unit is mainly exposed in the depocentres of the Polemi, Pissouri and Psematismenos/ Maroni basins; it is characterized by a welldeveloped cyclicity, given by the alternation of sapropel, marl, and carbonate beds, suitable for an integrated stratigraphic approach. For this purpose, two sections were studied in detail: the Motorway section, in the Pissouri basin (Krijgsman et al., 2002) and the Tokhni section, in the Maroni/Psematismenos basin (Orszag-Sperber et al., 2009).

MSCunits

The Kalavasos Formation records the whole Messinian salinity crisis; it can be subdivided into three main subunits (Rouchy, 1982; Robertson et al., 1995; Orszag-Sperber et al., 2009), that are from the bottom: (i) the Lower Gypsum; (ii) the Intermediate breccia; and (iii) the Lago-Mare deposits and Upper Gypsum (Fig. 4).

The Lower Gypsum unit, up to 70 m thick (Robertson et al., 1995), is described as a composite unit including a large variety of gypsum deposits: selenitic, laminar (locally known as 'marmara' gypsum), clastic and nodular (Rouchy, 1982). A discontinuous unit known as 'barre jaune', a carbonate breccia including stromatolitic deposits and fragments of primary gypsum (Rouchy, 1982; Orszag-Sperber et al., 2009), is commonly present at the base of the lower unit (Fig. 4).

The Intermediate Breccia, up to 20 m thick (Robertson et al., 1995), is a polygenic and heterometric breccia made up of gypsum clasts and blocks in a carbonate/gypsarenite matrix (Rouchy, 1982). According to Robertson et al. (1995) the gypsum clasts derive from different gypsum facies including both twinned selenite crystals and laminar gypsum. According to these authors this 'mega-rudite' unit resulted from large-scale tectonically induced mass-failure.

The Upper Gypsum unit, up to 60 m thick (Robertson et al., 1995), is lithologically very variable. According to Rouchy (1982), this unit includes up to six gypsum beds characterized by different facies; mainly selenitic in the lower three beds, and mainly laminar gypsum associated with clastic and minor selenitic gypsum in the upper three-ones. These gypsum beds are separated by marl horizons characterized by the presence of the typical Lago-Mare brackish faunal assemblages (Roveri et al., 2008a and references therein) of Parathetyan affinity, including mollusks (Limnocardiine, Melania, Melanopsis), ostracods (Cyprideis) and foraminifers (Ammonia beccarii). In the Pissouri area the interval comprised between the uppermost gypsum bed and the Messinian-Zanclean boundary consists of a lower marl unit with Lago Mare ostracods and gastropods capped by an alternation of conglomerate, calcarenites and paleosoils (Rouchy et al., 2001). Conglomerate clasts mostly derived from the Lefkara and Pakhna limestones, together with Troodos sourced volcanic pebbles also occur for the first time in the southern Cyprus basins (Rouchy et al., 2001), thus, suggesting a significant uplift phase of the Troodos massif.

MATERIALS ANDMETHODS

We have investigated the stratigraphic interval encompassing the upper portion of the Pakhna Formation and the evaporites of the Kalavasos Formation, up to the base of the Pliocene. Our study is mainly based on the facies analysis of several sections outcropping in the Psematismenos/ Maroni, Polemi, Pissouri and Mesaoria basins (Fig. 2; see also supplementary file). Moreover, we have performed biostratigraphic (planktonic foraminifera and calcareous nannofossils) and petrographic analyses of the upper Pakhna Formation in the Tokhni section (Maroni/ Psematismenos basin) and strontium isotope analysis of samples from the evaporites of Kalavasos Formation.

Bio-magneto-stratigraphy

An integrated bio-magneto-stratigraphic study of the upper part of the Pakhna Formation exposed in the Tokhni section (Figs 4 and 5) including a semi-quantitive biostratigraphic analysis of planktonic foraminifer assemblages and a detailed smear-slide quantitative study of calcareous nannofossils assemblages has been undertaken and will be published in a

separate work (R. Gennari, F. Dela Pierre, F.Lozar, E. Turco, S. Lugli, V. Manzi, M. Natalicchio, M. Roveri, M. Taviani, unpublished data.). In this paper we have included only some qualitative observations emerging from that study.

Petrographic analyses
Carbonates
Nine standard thin sections of carbonate rocks from Tokhni and Pissouri sections were studied with transmitted light and were further analyzed for their UV-fluorescence on a Nikon microscope with a UV-2A filter block, using ultraviolet light (illumination source 450–490 nm). Scanning electron microscopy and qualitative element recognition were performed with a Cambridge Instruments Stereoscan 360 scanning electron microscope equipped with an energy-dispersive Link System Oxford Instruments microprobe on 10 stubs from Tokhni section. Some selected thin sections were stained with alizarine to distinguish the dolomitic component.
Gypsum
We performed standard thin section analyses on the petrographic microscope.

Strontiumisotope analyses
Sr isotope analyses were carried out at Scottish Universities Environmental Research Centre, East Kilbride, Scotland (SUERC). Samples were leached in 1 M ammonium acetate prior to acid digestion with HNO_3. Sr was separated using Eichrom Sr Spec resin. Matrix elements were eluted in 8 M HNO_3 and 3 M HNO_3 before elution of Sr in 0.01 M HNO_3. Total procedure blank for Sr samples prepared using this method was <200 pg. In preparation for mass spectrometry, Sr samples were loaded onto single Re filaments with a Ta-activator. Sr samples were analyzed with a VG Sector 54–30 multiple collector mass spectrometer. A $_{88}Sr$ intensity of 1 V (1 9 10^{-11} A) _ 10% was maintained. $_{87}Sr/_{86}Sr$ ratio was corrected for mass fractionation using $_{86}Sr/_{88}Sr = 0.1194$ and an exponential law. The mass spectrometer was operated in the peak-jumping mode with data collected as 15 blocks of 10 ratios which gives an internal uncertainty of <0.000020 (2 SE). For this instrument NIST SRM 987 gave 0.710249 _ 0.000008 (1 SD, n = 17) during the course of this study. The 2 standard error internal precision on individual analyses was between 0.000014 and 0.000020 for 2r.

NEWDATA AND OBSERVATIONS FROM MESSINIAN SUCCESSIONS
Psematismenos/Maroni basin
The reconstruction of the stratigraphic framework for the Psematismenos/Maroni basin is based on observations on multiple sections (see locations in Fig. 5c).
The pre-MSC succession (Pakhna Formation)
The upper part of the Pakhna Formation crops out, in the badlands 1 km southwest of the Tokhni village, where it is overlain by the evaporites of the Kalavasos Formation. Here we measured the Tokhni composite section that includes 4 subsections (Fig. 5), which, from north to south, have been called, respectively, To-0, To-1, To-2 and To-3.
Facies analyses allowed the subdivision of the Pakhna Formation into a marly member (PK-A) and a carbonate member (PK-B).
Marly member (PK-A) – This member is largely made up by shale and marl, and limestone is a minor component; from the base, it shows three subunits: PK-A$_1$, PK-A$_2$, PK-A$_3$.
The lower part of the succession (subunit PK-A$_1$; Fig. 5) consists of a m-thick alternation of darker and lighter intervals of homogeneous blue marls. In the upper part of this unit the Tortonian-Messinian boundary has been recognized (Orszag-Sperber et al., 2009). The boundary with the overlying unit (subunit PK-A$_2$; Figs 5 and 6) is sharp and corresponds to the onset of m-thick layers of whitish marl interbedded with the blue marls.
An 80 cm-thick whitish limestone bed marks the base of the third unit (subunit PK-A$_3$; Figs 5 and 7a), which consists of a cyclical alternation of reddish marls and whitish micritic limestones. The micritic limestone layers are laterally continuous, in particular the lowermost one, and easily traceable along the outcrop so they have been used as key-beds in the reconstruction of the composite section (Fig. 6). The limestone layers are made up of a mixture of clay and coccoliths cemented by micron-sized calcite crystals. No dolomite has been found in the samples (Fig. 8f).
In the upper part of the section, two reddish diatomite layers and a thin (25–40 cm) conglomerate layer, consisting entirely of limestone-derived pebbles are key beds that facilitate correlation of the three subsections.
The basal part of the Tokhni section (Tortonian) contains at places holoplanktic mollusks, such as pteropods (Cavolinia gypsorum) and sparse deep-water benthic taxa such as the deep-water pectinid Propeamussium duodecimlamellatum (also reported by Merle et al., 2002). The macrofaunal component hosted in the overlying Messinian
carbonate marls is richer and more diverse, including bivalves, gastropods and occasional echinoids. This macrofauna is best observed in the Pakhna Formation of the Pissouri basin, described in the following chapter.
Carbonate member (PK-B) – This member is largely made up of limestone with a minor shale component and lies conformably above the unit PK-A$_3$.
PK-B unit (fig. 5 and 7), recognized only in the southern subsections To-2 and To-3, consists of 3 limestone beds (beds A, B and C in Fig. 6) previously described by Orszag-Sperber et al. (2009). Bed A (Fig. 8a) is bipartite, with a lower laminar and an upper chaotic portion separated by a sharp surface. The lower part consists of a sub-mm alternation of dark peloidal micrite and whitish carbonate laminae (Fig. 8c). The latter are composed of clotted micrite containing curved filaments up to 30 lm across (Fig. 8d). The micrite encloses irregular cavities, 80–200 lm in size, filled with microspar (Fig. 8d). In the upper part of bed A (Fig. 8b), the laminae are broken, deformed and reworked in three main

horizons. This fabric suggests the penecontemporaneous and almost in place reworking of the microbialite by subaqueous unidirectional currents.

The upper two layers (B and C) show completely different characteristics and internal organization. They are composite beds characterized by a chaotic brecciated division sandwiched between two laminated grainstone layers, coarse-grained below and fine-grained above; these beds can be interpreted as slurry-beds, i.e. deposits that accumulated rapidly from a flow that was transitional between a debris flow and a turbiditic flow (Lowe & Guy, 2000) and that maintained a chaotic division. The chaotic portion includes blocks and rip-up clasts of whitish micritic limestones (Fig. 7c, d). Observations at the microscope suggest that the grainstones and rudstones mainly consist of intraclasts coated by laminated rims of clotted micrite of probable microbial origin. The same rim is present, coating skeletal grains such as worm tubes (Fig. 8e). These sedimentological and petrographical features suggest that these carbonate beds were deposited by gravity flows.

Qualitative micropaleontological observations in the Pakhna show that the planktonic foraminifera are discontinuously present along the section and disappear just above bed A (Fig. 5), while benthic foraminifera (mainly Bolivina and Bulimina genera) last occurrence is observed immediately below bed B. Calcareous nannofossils, fairly abundant in the section, are also present above bed A with abundant and monospecific assemblages (Umbilicosphaera rotula), but disappear above bed B (Fig. 5). The marl interval between beds B and C contains cuspidariid bivalves, i.e. Tropidomya aff. abbreviata (Forbes, 1843) and Cardiomya aff. costellata (Deshayes, 1835). These bivalves (Fig. 9) suggest an outer shelf/slope depositional muddy environment in all likelihood substantially deeper than 100 m (e.g. Sturani, 1976;Merle et al., 2002).

Orszag-Sperber et al. (2009) interpreted these carbonate layers as microbialites formed at very shallow depth (stromatolites), that were eventually subjected to subaerial exposure based on the inferred presence of desiccation cracks and tepee structures.

Clotted fabric of micrite and the occurrence of filaments, likely representing remains of microbes, observed in the lower part of bed A actually support a microbial origin for these deposits. However, we have found no evidence of shallow water or subaerial exposure in these layers. Moreover, on the basis of the clastic facies recognized in the carbonate beds (in the upper portion of bed A and in whole B and C beds), we suggest that these deposits derive from the dismantlement of a penecontemporaneous carbonate platform or ramp, probably deveoped above structural highs surrounding the Tokhni area, and their resedimentation in relatively deeper (epi-bathyal) waters.

Macrofaunal data from intervening marls lend support to this hypothesis suggesting an outer shelf/upper slope depositional setting.

These carbonates record the onset of stressed environmental conditions, favouring the growth of microbial mats at the sea bottom, not necessarily at shallow water depth or under subaerial conditions. This interpretation is also suggested by the presence of monospecific calcareous nannofossil assemblages.

The evaporites (Kalavasos Formation)

The Kalavasos formation has been studied not only in the Tokhni section, but also in other sections outcropping between the villages of Tokhni and Psematismenos (Figs 2c and 5c).

In the Maroni/Psematismenos basin the boundary between the Pakhna and Kalavasos formations is sharp and characterized by an angular unconformity. A careful observation of the uppermost part of the Pakhna Formation in the Tokhni section, from section To-2 to To-0, shows: (i) an homogeneous NW dip (8°) of the Pakhna formation; (ii) the disappearance of the PK-B member; (iii) the progressive truncation of the carbonate beds of the PK-A$_3$ member (Figs 5 and 6); and (iv) an angular discordance of approximately 7° characterized by a steeper inclination of the base of the Kalavasos evaporites (15°) with respect to the Pakhna Formation (8°). All these elements indicate that the base of the evaporites is an angular unconformity associated with an indeterminable hiatus. Moreover, the Lower unit of the Kalavasos Formation consists exclusively of clastic evaporites derived from the dismantlement of primary evaporites. The MSC evaporites in the Maroni/Psematismenos basin can be separated into three main units.

The Lower unit includes several clastic gypsum facies (Fig. 10). The lowermost portion cropping out in the To-0 subsection consists of a composite bed (Fig. 10a) around 4 m-thick, formed by: (i) a 2 m thick lower chaotic division with an irregular and erosional base consisting of a mixture of gypsum blocks with banded and massive selenite, sparse selenite crystals in a shale and carbonate matrix derived from the underlying Pakhna Formation; (ii) a 25 cm-thick gypsrudite division showing normal gradation and traction carpets of clay and carbonate clasts; and (iii) a 1.5 m thick, normally graded gypsarenite division with a basal sharp bypass surface and characterized by parallel and ripple cross-lamination. This composite megabed is overlain by a 3–4 m thick interval with an overall fining-upward trend, exposed in the Tokhni and in the Psematismenos quarries, including gypsrudite, gypsarenite and gypsiltites in dm to m-thick beds, each one showing normal gradation, cross-lamination and hummocky cross-stratification in the upper portion of the beds. In the Psematismenos quarry well-preserved fossils of the hyperhaline crustacean Artemia salina (Figs 10b and 11a) have been found in a whitish gypsiltite interval at the top of a gypsarenite bed with hummocky crossstratification (Fig. 10e). In the Tokhni quarry, gypsum cumulate laminites are found in the upper part of the unit (Fig. 11). Gypsum cumulates are made up of acicular crystals up to 1.5 mm in size; less common whitish laminae consisting only of coarser crystals, are alternated with composite brownish laminae, more rich in carbonate and organic matter, formed by finer crystals (Fig. 11b, c). Gypsum cumulates, that formed at the pycnocline interface and then settled down and accumulate to the bottom, could have been deposited at any bathymetry.

Anyway, in this case bird foot prints (Fig. 10c), recognized in a gypsiltite/arenite bed in the uppermost part of the unit, suggest deposition in a very shallow-water environment during the acme of the Messinian salinity crisis.

The Intermediate unit is again a chaotic unit with a maximum thickness of 3 m (measured in the Tokhni gypsum quarry) that, differently from the previous one, consists almost exclusively of fragments of cumulitic gypsum laminae (the so-called 'marmara' variety).

The Upper unit consists of a metric alternation of gypsum and shale beds. Three gypsum/shale couplets have been recognized along the old road parallel to the highway (Fig. 5c; section UG). The gypsum beds show a completely different facies from the underlying deposits, being largely formed by bottom-grown gypsum selenite and subordinately by cumulate deposits. A more detailed description of this unit has been obtained from the sections of the Polemi basin, where this unit crops out more extensively.

Polemi basin: the Kallepya-Lethymbou- Polemi composite section

A more complete succession of the Kalavasos Formation exposed in the Polemi basin allowed a detailed study of the vertical and lateral facies changes in the MSC units; similar to the Maroni/Psematismenos basin this formation has been subdivided into three subunits (Fig. 12).

The Lower unit is 30–40 m-thick and consists of clastic evaporite deposits. A chaotic unit, consisting of a carbonate breccia locally including clasts of primary shallow-water bottom grown selenite (Fig. 13a), is commonly present in its lowermost portion; it corresponds to the so-called 'barre jaune' (Rouchy, 1982; Orszag- Sperber et al., 2009). This chaotic unit, characterized by an erosional basal surface and abrupt lateral thickness changes, lies unconformably over the barren interval of the uppermost Pakhna Formation, which records a progressive upward depletion of foraminifera. The chaotic unit is capped by a clastic gypsum unit which includes gypsrudite, gypsarenite and gypsiltite beds emplaced by subaqueous low-density gravity flows (Fig. 13b, c, f). These beds, showing erosional base, normal gradation, and traction-plus-fallout structures (climbing ripples) are alternated with laminar gypsum intervals (lg; Fig. 13b, d). This laminar gypsum variety is locally known as 'marmara'; it can be easily broken into flat slabs and for this reason it is exploited in quarries, which represent the main outcrops. It is formed by thin-bedded (mm to cm) primary cumulate laminae separatedby thin carbonate and organic matter veneers (Fig. 13b, e). Like in the Tokhni quarry section, the gypsum cumulates are formed by an alternation (Fig. 11d, e) of whitish (coarser crystals) and composite brownish laminae (more rich in carbonate and organic matter, formed by finer crystals). The whitish/brownish alternation would possibly reflect pluri-annual salinity fluctuations of the brines, as larger crystals could be the results of a reduced number of crystallization nuclei, which grow larger, compared to the finer crystals. The coarser laminae contain locally whitish nodules made up of cm-long gypsum prisms. They grow displacively, deforming the brownish cumulate laminae. Locally, the latter drape the nodules, thus suggesting a very early formation.

The Intermediate unit can be observed in small outcrops and consists of chaotic intervals derived almost exclusively from the resedimentation of the gypsum cumulate facies (marmara variety). A thickness of 10– 15 m has been estimated.

The Upper unit consists of up to six primary gypsum beds (UG1–UG6; Fig. 12), with thickness ranging between 1 and 6 m, alternating with poorly exposed intervals of beige and grey marls and marly limestones. The overall thickness of this unit has been estimated at around 50–60 m (Rouchy, 1982), although lateral thickness variability, mainly related to syn-depositional tectonic features, has been observed. The contact with the underlying unit is apparently discordant and the lowermost gypsum beds (UG1) onlap against the 'marmara chaotic' interval (Figs. 14a, b). This contact is probably related to the irregular topography created by the chaotic unit rather than a tectonic discordance, as witnessed by the absence of significant change in bed attitudes between the Lower and the Upper units.

It is worth noting that the vertical organization of this unit remains quite constant throughout the Polemi basin (Lethymbou, Polemi and Stroumbi sections) in terms of stacking pattern and evaporites facies distribution (Figs 12 and 14). UG1 is a 4–5 m thick gypsum bed entirely composed of banded selenite deposits showing minimal variability in crystal size. UG2 is the thickest bed (up to 6 m) and consists of a lower portion (3–4 m) with large twinned crystals overlain by a banded selenite facies. Fish remains of Aphanius crassicaudus (G. Carnevale, pers. comm.; Fig. 15), a taxon largely found in the Messinian units (see Carnevale et al., 2006 and reference therein), have been recognized in the marls below this bed east of Lethymbou. UG3 starts with about 1 m of whitish laminar gypsum, with granular cumulate alternated to thin selenite crusts, capped by a gypsarenite bed of similar thickness. UG4 starts with 70 cm-thick gypsrudite and gypsarenite layer capped by 1 m-thick laminar gypsum interval, similar to the one of the bed UG3, in turn overlain by a 2–3 m thick, banded selenite bed. UG5 is a 4 m-thick, banded selenite bed sandwiched between 2 laminar gypsum intervals, 1 m-thick each, again showing granular cumulate and subordinate thin selenite crusts. UG6 is the thinner bed, 1 m-thick, consisting of whitish gypsum formed by mm- to cm thick laminae. The laminae are made up of graded, granular gypsum crystals up to 0.3 mm in size. Cyprideis and Ammonia are present in the shales below bed UG6, whereas abundant mollusc remains are found at the top of the bed and intercalated with the laminae (Figs 12 and 15). Burrows filled by gypsiferous greenish mud are locally present.

This fossil fauna is relatively diverse and includes limnocardiine (e.g. 'Pontalmyra'spp.) and Dreissena bivalves, and gastropods such as hydrobiaceans (Saccoia) and Melanopsis narzolina. Biosomes are preferentially, but not exclusively, found in the laminar interface and bivalves are mostly articulated. This fauna is compositionally somewhat similar to post-evaporitic Lago-Mare assemblages from other sites in the Messinian Mediterranean basin (e.g. Esu & Taviani, 1989; Esu, 2007; Taviani et al., 2007; Esu & Girotti, 2008; Guerra- Merchan et al., 2010; Angelone et al., 2011;).

Regarding Cyprus specifically, Rouchy et al. (2001) report a relatively diverse Lago-Mare gastropods and ostracod fauna, and Characeae from a 25-m-clayey interval between the UG6 bed and the base of the Pliocene in the Polemi basin (Giolou section). These authors also mention abundant Limnocardiidae and Melanopsis fromgypsified algal laminites linked to the uppermost gypsum layer, a situation very similar to UGS 6. Ecologically, the gypsum-embedded fauna could possibly document a short-lasting shallow water anomalohaline water body; however, habitable by these mollucs. Possibly due to an increase in evaporation, this habitat somehow suddenly reverted into evaporitic conditions, likely lethal to anomalohaline biota whose shells got then entrapped in the gypsum.

According to Rouchy et al. (2001) a clayey interval of around 25 m in thickness rich in Lago-Mare gastropods, ostracods and charophyte remains, is present between the UG6 bed and the base of the Pliocene in the Polemi basin (Giolou section). In the few metres encompassing the Messinian-Zanclean boundary exposed along a dirt road south of the Polemi Village, above UG6, we observed a 1.5 m thick massive sandstone bed, that overlays a poorly exposed paleosol, capped by 1 m of grey clays containing in its upper part an ostracod assemblage including Loxocorniculina djafarovi, Euxynocythere praebaquana and C. agrigentina, mixed with reworked Eocene and Miocene foraminifers. This ostracod assemblage is typical of the uppermost Lago-Mare phase (Gliozzi & Grossi, 2008). A dark, organic-rich layer separates this uppermost Messinian deposits from the whitish Lower Pliocene marls characterized by open marine foraminifera. This dark layer yields Lago-Mare fauna (C. agrigentina), Pliocene planktonic foraminifera and Miocene to Eocene reworked planktonic foraminifera; this is probably the result of the bioturbation observed in the field affecting its uppermost part. It closely resembles a similar layer described in the Northern Apennines (Gennari et al., 2008) at the Miocene- Pliocene boundary. The basal Pliocene marls only yield foraminifera, mainly planktonic (mainly Globigerinoides spp. and Orbulina universa); the occurrence of Neogloboquadrina acostaensis destral coiled and the absence of Sphaeroidinellopsis and Globorotalia margaritae suggest the occurrence of the basal MPl1 biozone.

Pissouri basin: the Pissouri section

The pre-MSC unit and the onset of the Messinian salinity crisis

A nearly complete Messinian succession extending from the upper Pakhna Formation up to the Zanclean crops out in the Pissouri basin. Due to the well-expressed lithological cyclicity, the pre-evaporitic succession has been studied in detail in the Pissouri Motorway section (Krijgsman et al., 2002; Kouwenhoven et al., 2006; Morigi et al., 2007) that represents a reference section for the definition of the onset of the Messinian salinity crisis in the Eastern Mediterranean. In order to compare the onset of the evaporites observed in the Maroni/Psematismenos and in the Polemi basins, we focused on the uppermost portion of the Pissouri Motorway section, precisely from cycle 5 of Krijgsman et al. (2002) upward (Fig. 16) that according to these authors lacks robust chronostratigraphic constraints because no bio- or magnetostratigraphic events have been clearly identified.

After a stratigraphic and sedimentological revision of the section we suggest as showed in Fig. 16, that the onset of the MSC is not present and that a clastic eveporite unit rests unconformably on the pre-MSC deposits of the Pakhna formation. Our interpretation is based on the following observations.

· The chaotic bed described in Krijgsman et al. (2002) is sandwiched between two carbonate layers that have been correlated with two insolation minima. In our opinion this interval cannot be considered for astronomical tuning purposes because both the chaotic and the indurated bed at its top (cycle 3 of Krijgsman et al., 2002) were emplaced by a gravity flow and thus in a geologically instantaneous event. In our opinion, the latter is actually a mixed, carbonate and siliciclastic, graded bed (Fig. 16c) genetically associated with the slump.

· The slump interval includes slabs of a carbonate bed similar to those present below it, but moving 100− 150 m toward NE a large (up to 8 m high and a few tens of m large) reefal limestone block is also present; in our interpretation this block been transported from an adjacent topographic/structural high following the dismantlement of a shallow water carbonate platform.

· Only two of the carbonate beds used by Krijgsman et al. (2002) for the definition of the lithological cycles between cycle 3 and the base of the evaporites have a thickness similar to the beds below the slump. Moreover, they are clastic carbonates (Fig. 16d) showing clear evidence of transport by unidirectional currents and emplaced by geologically instantaneous gravity flows. This is similar to what observed in the Tokhni section, where the uppermost portion of the pre-evaporitic formation is characterized by the presence of clastic carbonate deposits. Unfortunately, no suitable bio-magnetostratigraphic constraints occur in this portion of the section (Krijgsman et al., 2002).

· The evaporite unit is not composed of in situ primary evaporites, but of a sedimentary chaotic unit, several tens of metres thick, including carbonate breccias, reefal carbonate blocks, gypsrudite with pebbles of primary shallow-water selenite, and blocks of cumulate and clastic gypsum (Fig. 16e, f). This chaotic unit is capped by 8−10 m of gypsrudite and gypsarenite graded beds; on top of these, 6−8 m of yellowish laminated fine calcarenites and massive limestones are present below the lowermost local shallow-water in situ selenite bed attributable to the Upper gypsum unit.

· Even if the age of the chaotic gypsum unit cannot be defined, the presence of branching selenite (Lugli et al., 2010) blocks, which first appearance in the Western Mediterranean has been reported only from PLG cycle 6th upwards, suggests that the chaotic could be significantly younger than the MSC onset.

Furthermore, if we consider that (i) the succession below the chaotic megabed is older than 6.1 Ma (Krijgsman et al., 2002); (ii) the C3An.1n normal chron lasted 10 precessional cycles (Sierro et al., 2001); and that (iii) only two possible

lithological cycles are present above the chaotic megabed, thus, a different tuning (Fig. 16) implying the presence of a hiatus of undetermined duration at the base of the chaotic gypsum can be proposed.

If our stratigraphic interpretation is correct, the base of the evaporites in the Pissouri basin does not correspond with the basin-wide onset of the Messinian salinity crisis, but it represents a regional-scale erosional surface eroding the deposits accumulated during the stage 1 of the MSC, either PLG or their deep water evaporite-free time equivalent, that were no longer preserved in situ in this area. Consequently, we suggest that the first evaporite unit corresponds to the Resedimented Lower Gypsum unit (RLG, Roveri et al., 2008a,c) and the surface at its base, to the Messinian erosional surface (MES).

Mesaoria basin:Kato Moni section

Kato Moni is the only section that we have studied in the Mesaoria basin, in the northern side of the Troodos Massif (Fig. 1). In the Kato Moni area (Fig. 17a) an angular unconformity between the Pakhna and the Kalavasos Formation has been recognized (Follows, 1990; Robertson et al., 1995). The main outcrop of Messinian evaporites is located in a small abandoned quarry (Lat $35°3_0 49.20''$ N, Lon $33°6_0 4.01''$ E) located 1 km east of Kato Moni (Fig. 17b). Here, in a 20 m-thick succession (Fig. 17c), we have recognized four gypsum beds separated by very thin (few dm thick) shale intervals. Each gypsum bed is bipartite: the lower part is thinner (1−2 m-thick) and consists of cumulate gypsum in sub-centimetric laminae (Fig. 17d), the upper part is thicker (3−4 m-thick) and made up of massive or banded selenite, grown in situ. On the basis of facies analogies, overall thickness and stacking pattern of the evaporites exposed in the Maroni/Psematismenos, Pissouri and Polemi basins and the occurrence of the unconformity at the base of the evaporites, we suggest that this unit corresponds to the Upper Gypsum unit and the basal unconformity corresponds to the Messinian erosional surface (MES).

Mesaoria basin:Xeri borehole (Gass,1960)

Further data on the MSC of the Mesaoria basin can be obtained from literature. The Xeri borehole (Fig. 18; Gass, 1960; located few km SW of Nicosia, approximately at LAT $35°6_0 44''$ N, LON $33°18_0 21''$ E; Robertson et al., 1995) describes a tripartite evaporite unit with a total thickness of ca. 500 m capped by a Pliocene grey marl unit containing shells fragments. From the bottom it includes: (i) a basal 60 m-thick grey marls unit containing anhydrite; (ii) a ca. 290 m-thick salt unit consisting of three pure salt intervals separated by two thin marl horizons (for which a total thickness of 9 m was estimated); and (iii) ca. 100 m-thick grey marl unit containing gypsum, carbonate and igneous rock fragments. In our opinion this units can be regarded as the Upper Gypsum unit succession cropping out along the southern margin of the Mesaoria basin.

Strontiumisotopes

The $_{87}Sr/_{86}Sr$ isotope ratio has been measured on six gypsum samples (Table 1); their values are plotted in Fig. 19 against coeval global ocean values and the general trend for the MSC as recently compiled by Roveri et al. (2014b) that provided a complete recalibration of the Messinian evaporites Sr values based on sedimentologic and stratigraphic review of the MSC record.

Two samples have been collected in the lower clastic units of the Kalavasos Formation: one in a block of primary selenite in the Pissouri section, and a second one in the brine shrimp-bearing gypsiltite of the Psematismenos quarry (Maroni/Psematismenos basin). They provided very similar values (0.708951 and 0.708966, respectively; error _ 0.00002) that plot very close to the field of the global ocean (Flecker et al., 2002; Flecker & Ellam, 2006) and show the typical signature of the Primary Lower Gypsum deposits (Lugli et al., 2010; Roveri et al., 2014b). This suggests that the clastic units made up by recycled primary shallow water gypsum deposited during the first stage of the Messinian salinity crisis. Conversely, four samples from the Upper Gypsum unit, collected in the lowermost and in the uppermost cycles (Table 1) provided values unequivocally lower than the previous ones that (0.708795 _ 0.708866 _ 0.00002) that plot in the field of the Mediterranean Upper Evaporites (Roveri et al., 2014a).

DISCUSSION

In their paper, Orszag-Sperber et al. (2009) conclude that "the onset of the massive evaporites" in Cyprus basins was anticipated by an important event "represented by chaotic formations and/or by episodes of desiccation and development of shallow water microbial carbonates communities" that "records a significant drop of the water level that predated the deposition of the lower gypsum." Moreover the authors argued that "reworking of large blocks primary gypsum" in the barre jaune unit "indicates that the onset of the massive gypsum precipitation is not exactly coeval in the different basins from Cyprus and thus at the Mediterranean scale".

Our new observations and data suggest a different reconstruction of Messinian events in Cyprus.

Useful stratigraphic tools for the definition of theMSConset, in Cyprus-

Our study of the pre-MSC succession reveals that in the Cyprus basins the onset of the Messinian salinity crisis cannot be easily defined. The lower Messinian Pakhna Formation is generally characterized by hemipelagic sediments with a well-developed lithological cyclicity, which has been astronomically tuned in previous studies providing an age estimation of the onset of MSC (Krijgsman et al., 2002; Kouwenhoven et al., 2006; Morigi et al., 2007; Orszag-Sperber et al., 2009). Conversely, the uppermost portion of the Pakhna Formation (carbonate member, PK-B) is dominated by clastic carbonate deposits. As a consequence the cyclostratigraphic approach should be used with caution to avoid errors

in the age estimate of the MSC onset that could produce an apparent diachroneity of this event (see discussion in Manzi et al., 2011).

Alternatively, we suggest to use palaeoenvironmental and palaeocenographic proxies to define the onset of the MSC. Thus, on the basis of the last occurrence of planktonic foraminifera (Fig. 6) the carbonate layers B and C of the Tokhni section could be considered as time-equivalent of the lowermost stage 1 primary evaporites (PLG).

The onset of the evaporites vs. the onset of Messinian salinity crisis in Cyprus

The study of the evaporites of Cyprus reveals that no in situ shallow-water primary selenites similar to those deposited during the stage 1 of the MSC (PLG; sensu Roveri et al., 2008a,c) either in the Western and in the Eastern Mediterranean (Greece; Karakitsios et al., 2013), are preserved in the Cyprus basins; instead a composite 'Lower Evaporite' unit mainly consisting of gypsrudite and gypsarenite emplaced by gravity flows occur above the lower Messinian pre-MSC deposits.

A carbonate unit named 'barre jaune' (Rouchy, 1982) commonly, but not always, is present at the base of the Lower Evaporites; this unit has been usually considered to mark the onset of the Messinian salinity crisis (Rouchy, 1982; Krijgsman et al., 2002; Kouwenhoven et al., 2006; Morigi et al., 2007) or to record a significant sea level drop anticipating the MSC onset (Orszag-Sperber et al., 2009). Actually this unit is a carbonate breccia including gypsum clasts and blocks (see description of the Kallepya and Tokhni sections), showing high lateral thickness variability. In our interpretation, this is not a clastic unit preceding the onset of the MSC (Orszag-Sperber et al., 2009), but a chaotic unit vertically and laterally associated with clastic gypsum deposits of the Lower unit. The base of this composite clastic unit, including both carbonate and gypsum, is a regional-scale unconformity showing a strong erosional character and locally associated with an angular discordance (see Tokhni section). Thus the base of the evaporites in Cyprus does not represent the onset of the salinity crisis in the Mediterranean that is instead preserved in deep-water evaporite-free deposits of the uppermost Pakhna Formation and marked by the disappearance of foraminifera, as documented elsewhere in the Mediterranean (Manzi et al., 2007, 2013; Dela Pierre et al., 2011; Gennari et al., 2013).

The origin of Cyprus evaporites

The evaporite suite of Cyprus includes primary, both cumulate and bottom grown, and clastic deposits.

The in situ bottom-grown facies are found exclusively in the Upper Gypsum unit, whereas the Lower Gypsum unit includes only clastic and cumulate facies. This overall organization is the same of that described for the intermediate basins of the Mediterranean (Roveri et al., 2014b), i.e. basins at an intermediate depth, roughly between 200 and 1000 m, that were too deep to allow the deposition of bottom-grown selenite, but that were not the deepest basins in the Mediterranean.

Strontium isotopes obtained from the clastic unit (see previous paragraph; Fig. 19) indicate their deposition during the first stage of the Messinian salinity crisis, when the Mediterranean water body was still only slightly diluted by continental input (Roveri et al., 2014a,b). Consequently, we suggest that all together the 'barre jaune' and the clastic gypsum of the Lower Unit can be ascribed to the Resedimented Lower Gypsum unit (RLG; sensu Roveri et al., 2008a, 2014b) of the Western Mediterranean ad belonging to the stage 2 of the MSC. Our data (Fig. 20) testifies the erosion and the resedimentation of shallow water bottom-grown selenite deposits of MSC stage 1 that were probably located on structurally more elevated basins, maybe above the Troodos massif that, according to the presence of late Tortonian-early Messinian reef units (Koronia member) boarding it to the south and to the north (Follows et al., 1996), could have been located at shallow water at those time. These primary evaporites have been successively uplifted and eroded following a phase of tectonic activity. This could be possibly related to late Miocene change in stress regime suggested by Kinnaird & Robertson (2013). Thus, the angular unconformity flooring the Lower Evaporites of the Kalavasos Formation of Cyprus does not represent the onset of the Messinian salinity crisis, but can be more reasonably correlated with the Messinian erosional surface, i.e. the base ofMSC stage 2.

In the upper portion of the Lower Unit of the Kalavasos Formation, in the Polemi basin we have observed an increase in cumulate gypsum facies ('marmara gypsum') with respect to the clastic ones. Moreover, the overlying intermediate unit is a chaotic deposit almost exclusively made up of cumulate and subordinately fine-grained clastic gypsum. This suggests a change in the depositional processes of the evaporites.

Initially, the bottom-grown selenites, deposited during the first stage of the MSC (PLG, sensu Roveri et al., 2008a,c), were eroded and resedimented by gravity flows. Their partial dissolution could have favoured the formation of higher salinity and denser brines able to sink and reach the bottom of the basin. This, in turn, could have resulted in a generalized increase of the salinity of the water mass and in a more efficient precipitation of cumulate crystals. A similar change in evaporite facies has been described in Sicily (Roveri et al., 2008a; Manzi et al., 2012) where the clastic gypsum, and carbonate deposits, are upward transitional to primary cumulate deposits, both of gypsum and halite. In our opinion the facies change observed in the Cyprus successions could have the same origin, thus suggesting that the deposition of the RLG could be associated with the deposition of the halite in the deeper portion of the Mesaoria basin. The chaotic marmara deposits suggest slope instability, possibly related to synsedimentary tectonic activity, which has been commonly observed in many other basins during MSC stage 2 (Roveri & Manzi, 2006).

Finally, based on facies analysis and strontium isotope ratio the Upper Evaporite unit can be clearly correlated with the Upper Gypsum unit that accumulated during stage 3 of the Messinian salinity crisis in Sicily (Manzi et al., 2009). This helps to constrain the age of the resedimented gypsum and associated halite and gypsum cumulates.

Sealevel drop associated with theMSC

An important sea level drop immediately preceding the onset of the Messinian salinity crisis has been envisaged by Orszag-Sperber et al. (2009) based on the recognition of shallow water and desiccation features in the three stromatolite-bearing carbonates underlying the massive evaporites and of large reworked fragments (in the 'barre jaune' of the Kallepya section, Polemi Basin).

Our observations suggest instead that these inferred stromatolites, are actually clastic carbonate deposited by subaqueous gravity flow, which do not show evidence of shallow-water deposition or subaerial exposure. Moreover, according to the fossil content of the intervening marls, these carbonates accumulated in an epi-bathyal depositional setting similar to the underlying deposits. This suggests that the onset of the MSC, approximately located on top of carbonate bed A in the Tokhni section (Fig. 5), is not associated with a significant sea level drop.

As for the Polemi basin, in our opinion the 'barre jaune' simply represents a lateral facies change in the clastic evaporites that are present in the basal part of the Lower Evaporite unit of Cyprus.

We propose that the base of the Lower Evaporites in all the Cyprus basins does not mark the onset of the MSC but corresponds to a regional-scale unconformity, whose formation is related to an important tectonic event that led to the erosion and resedimentation of the primary evaporites deposited during stage 1. This tectonic activity, that could have been related to an earlier phase of collision of the Cyprus Arc against the Eratosthenes microplate, could have resulted in the tectonic uplift of the Troodos Massif and in the reduction in the paleodepth of the surrounding basins, leading locally to conditions close to emersion, as suggested by the bird foot tracks recognized on top of the clastic evaporites in the Tokhni quarry. The local development within MSC stage 2 deposits of sedimentary features indicating short-lasting episodes of emersion (as found in the halite of Sicily; Lugli et al., 1999; Roveri et al., 2008a) is likely related to a combination of base-level drop, tectonic uplift and sedimentation rate of evaporites. It is worth noting that the ephemeral development and preservation of such shallow water environments in an uplifted area of marginal basins appears to be incompatible with a deep desiccation of the Mediterranean.

Eastern vs. western Mediterranean correlations

As observed in all the Cyprus basins, the Upper Gypsum unit seals the intra-Messinian tectonic phase. Unlike the underlying evaporites, they mainly consist of primary evaporite deposits alternating with shale/ marl intervals. These deposits are vertically arranged to form 6 lithological cycles that are entirely similar to the Upper Gypsum of Sicily and a tentative correlation is here proposed (Fig. 21). In comparison with the Upper Gypsum succession of Sicily, one evaporite cycle is apparently lacking in the Polemi basin. In the Polemi basin the Upper Gypsum unit shows a weak lateral variation in terms of evaporite facies, cycles number, stacking pattern and overall thickness. A terrigenous interval of variable thickness including 2–3 conglomerate beds and a similar number of paleosoils can be observed in both the Polemi and Pissouri basins in the uppermost part of the UG unit, below the Messinian- Zanclean boundary (see detailed description in Rouchy et al., 2001). This interval, containing fresh-water ostracod and mollusc assemblages typical of the Lago- Mare, resembles the terrigenous interval below the 7th gypsum bed in Sicily (Manzi et al., 2009) and could be tentatively correlated with the p-ev2 unit of the Northern Apennines (Roveri et al., 1998, 2001; Roveri & Manzi, 2006; Roveri et al., 2008a). If this correlation is correct the deposition of the gypsum in the precessional cycle preceding the M-Z boundary could have been hampered by local paleoenvironmental conditions, e.g. local higher runoff.

Is there anyway to constrain the timing of halite deposition in Cyprus and in the EasternMediterranean?

Unfortunately, the age of deposition of the main halite units during the MSC cannot be defined with absolute dating, thus, at the moment, waiting for a deep borehole crossing all the deep evaporite suites buried below the Mediterranean seafloor, the only possibility is to define a relative age adopting the stratigraphic constraints provided by the underlying and overlaying units. We have tried to put together all the stratigraphic data and to speculate on the possible solutions. The best place to try to face this problem in Cyprus is the basin extending from the onshore Mesaoria basin to its offshore continuation, the Larnaca-Latakia basin.

In the Mesaoria basin the presence of halite has been recognized by boreholes (Gass, 1960; Robertson et al., 1995; Fig. 18), whereas in the Larnaca-Latakia basin (Fig. 1) the presence of halite has been inferred from seismic profiles by (Robertson et al., 1995; Maillard et al., 2010). According to the seismic stratigraphic reconstruction provided by Maillard et al. (2010), the MU unit in the Larnaca-Latakia basin, mainly made up of halite, could be correlated with the thicker unit of the Levant basin. If we assume that no major hiatus ispresent in the halite unit drilled in the Mesaoria basin, a tentative correlation with the deep record of the Levant basin can be proposed (Fig. 22), correlating the main clastic intercalations that are present in the halite unit (Xeri Borehole; Gass, 1960) with some peculiar features seen in the seismic record, as the brittle layers of the Larnaka-Latakia basin (Maillard et al., 2010) or the high-amplitude reflector packages of the Levant basin (Gvirtzman et al., 2013), and tentatively tuned to astronomic curves (Roveri et al., 2014b; Fig. 22). Here we speculate that the MES in the onshore basins of Cyprus can be correlated with the surface at the base of the offshore evaporites (BES of Maillard et al., 2010), thus implying that the evaporite deposition in the deeper basin started only during the 2nd stage of the Messinian salinity crisis (5.6–5.55 Ma), as already proposed for the western Mediterranean (Lofi et al., 2005; Manzi et al., 2005; Hilgen et al., 2007; CIESM, 2008; Roveri et al., 2008a; Roveri et al., 2014a,b,c). Similar conclusions have been recently suggested also for the deeper part of the Eastern Mediterranean (Lugli et al., 2013).

CONCLUSIONS

A thorough revision of the uppermost portion of the preevaporitic succession (Pakhna Formation) and of the Messinian evaporites (Kalavasos Formation) cropping out in the Island of Cyprus confirms that the general Western Mediterranean stratigraphic framework (CIESM, 2008; Roveri et al., 2008a,c) also applies to this region of the Eastern Mediterranean. In particular our analyses reveal that:

· The pre-Messinian salinity crisis unit is truncated at the top by a regional-scale unconformity that lies at the base of the Cyprus evaporites;

· No shallow-water Primary Gypsum deposits (PLG; sensu Roveri et al., 2008a,c) have been preserved in situ; instead, laminated and clastic limestones have been observed;

· Primary Lower Gypsum deposits were probably deposited in more elevated basins (e.g. top of Troodos, Kyrenia) and were later dismantled and resedimented into the adjacent basins, where they have been preserved;

· The onset of the Messinian salinity crisis can be placed in the lower part of a gypsum-free unit clastic carbonate unit;

· During the erosion and resedimentation of the Primary Lower Gypsum unit a regional-scale unconformity, locally associated with an angular discordance, was produced in the shallower basins. It corresponds to the Messinian erosional surface (MES; sensu Roveri et al., 2008a,c) and can be traced at the base of the evaporites in the deeper basins;

· The Kalavasos evaporites can be separated into three units;

i The lower and the intermediate unit are mainly made up of clastic deposits and locally include halite (buried in the Mesaoria besin); they can be correlated with the Resedimented Lower Gypsum deposited in the Western Mediterranean during the 2nd stage of the Messinian salinity crisis (RLG; sensu Roveri et al., 2008a,c);

ii Resedimented Lower Gypsum deposits also can include (locally) very shallow-water deposits as demonstrated by bird tracks and the well-preserved layers of brine-shrimps and their moults seen in the Maroni section; no evidence of significant subaerial exposure has been found within this unit;

iii the Upper unit, containing up to six shallow-water primary selenite/marls couplets with typical Lago-Mare assemblages, corresponds to the Upper Gypsum unit (UG; sensu Roveri et al., 2008a,c) and have been deposited during the 3rd stage of the Messinian salinity crisis.

· We provided new sedimentological and stratigraphic data that can be useful to understand how the MSC was recorded in Eastern vs. Western Mediterranean and in shallow vs. deeper settings.

ACKNOWLEDGEMENTS

SUPPORTING INFORMATION

Additional Supporting Information may be found in the online version of this article:

Data S1. Location of the study sections.

Data S2. Location of the samples for strontium isotope analyses.

REFERENCES

AKSU, A.E., HALL, J. & YALTIRAK, C. (2008) Miocene-Recent evolution of Anaximander Mountains and Finike Basin at the junction of Hellenic and Cyprus Arcs, eastern Mediterranean. Mar. Geol., 258, 24–47.

ANGELONE, C., COLOMBERO, S., ESU, D., GIUNTELLI, P., MARCOLINI, F., PAVIA, M., TRENKWALDER, S., Van Den HOEK OSTENDE, L.W., ZUNINO, M. & PAVIA, G. (2011) Moncucco Torinese, a new post-evaporitic Messinian fossiliferous site from Piedmont (NW Italy). Neues. Jahrb. Geol. Palaontol. Abh., 259/1, 89–104.

BAGNALL, P.S. (1960) The geology and mineral resources of the Pano Lefkara-Larnaca area. Geol. Surv. Depart. Cyprus Mem., 5, 116.

BELLANCA, A., CARUSO, A., FERRUZZA, G., NERI, R., ROUCHY, J.M. & SPROVIERI, M. (2001) Transition from marine to hypersaline conditions in the Messinian Tripoli Formation from the marginal areas of the central Sicilian Basin. Sed. Geol., 140, 87–105.

BERNARDI, E. (2013) Integrated stratigraphy of the northernmost record of the Messinian salinity crisis: new insight from the

Tertiary Piedmont Basin. PhD Thesis, University of Turin, Italy.

BERTONI, C. & CARTWRIGHT, J.A. (2006) Controls on the basinwide architecture of the Messinian evaporites on the Levant margin (Eastern Mediterranean). Sed. Geol., 188–189, 93–114.

BERTONI, C. & CARTWRIGHT, J.A. (2007) Major erosion at the end of the Messinian Salinity Crisis: evidence from the Levant Basin, Eastern Mediterranean. Basin Res., 19, 1–18.

BLANC-VALLERON, M.M., PIERRE, C., CAULET, J.P., CARUSO, A., ROUCHY, J.M., CESPUGLIO, G., SPROVIERI, R., PESTREA, S. & di STEFANO, E. (2002) Sedimentary, stable isotope and micropaleontological records of paleoceanographic change in the Messinian Tripoli Formation (Sicily, Italy). Palaeogeogr. Palaeoclimatol. Palaeoecol., 185, 255–286.

BRIDGE, C., CALON, T.J., HALL, J. & AKSU, A.E. (2005) Salt tectonics in two convergent-margin basins of the Cyprus arc, Northeastern Mediterranean. Mar. Geol., 221/1–4, 223–259.

CALON, T.J., AKSU, A.E. & HALL, J. (2005) Varying tectonic control on basin development at an active microplate margin: Latakia Basin, Eastern Mediterranean. Mar. Geol., 221/1–4, 15–60.

CARNEVALE, G., LANDINI, W. & SARTI, G. (2006) Mare versus Lago-mare: marine fishes and the Mediterranean environment at the end of the Messinian Salinity Crisis. J. Geol. Soc. London, 163, 75–80.

CARTWRIGHT, J.A. & JACKSON, M.P.A. (2008) Initiation of gravitational collapse of an evaporitic basin margin: the Messinian saline giant, Levant Basin, eastern Mediterranean. Geol. Soc. Am. Bull., 120, 399–413.

CHAUMILLON, E., MASCLE, J. & HOFFMANN, H.J. (1996) Deformation of the western Mediterranean Ridge: importance of Messinian evaporitic formations. Tectonophysics, 263, 163–190.

CIESM. (2008) The Messinian salinity crisis from Mega-deposits to Microbiology. A consensus report. CIESM Workshop Monograph, 33, 168.

DELANGE, G.J. & KRIJGSMAN, W. (2010) Messinian salinity crisis: a novel unifying shallow gypsum/deep dolomite formation mechanism. Mar. Geol., 275, 273–277.

DELA PIERRE, F., BERNARDI, E., CAVAGNA, S., CLARI, P., GENNARI, R., IRACE, A., LOZAR, F., LUGLI, S., MANZI, V., NATALICCHIO, M., ROVERI, M. & VIOLANTI, D. (2011) The record of the Messinian salinity crisis in the Tertiary Piedmont Basin (NW Italy): the Alba section revisited. Palaeogeogr. Palaeoclimatol. Palaeoecol., 310, 238–255.

DELA PIERRE, F., CLARI, P., BERNARDI, E., NATALICCHIO, M., COST, E., CAVAGNA, S., LOZAR, F., LUGLI, S., MANZI, V., ROVERI, M. & VIOLANTI, D. (2012) Messinian carbonaterich beds of the Tertiary Piedmont Basin (NW Italy): microbially-mediated products straddling the onset of the salinity crisis. Palaeogeogr. Palaeoclimatol. Palaeoecol., 344–345, 78–93.

EATON, S. & ROBERTSON, A.H.F. (1993) The Miocene Pakhna Formation, southern Cyprus and its relationship to the Neogene tectonic evolution of the Eastern Mediterranean. Sed. Geol., 86, 273–296.

ESU, D. (2007) Latest Messinian "Lago-Mare" Lymnocardiinae from Italy: Close relations with the Pontian fauna from the Dacic Basin. Geobios, 40/3, 291–302.

ESU, D. & GIROTTI, O. (2008) The late Messinian Lago-Mare molluscan assemblage from the Trave Horizon (Colombacci Fm) at Pietralacroce (Ancona, Central Italy). Boll. Soc. Paleontol. Ital., 47/2, 123–129.

ESU, D. & TAVIANI, M. (1989) Oligohaline mollusc faunas of the Colombacci Formation (upper Messinian) from an exceptional fossil vertebrate site in the Romagna Apennines: monticino

Quarry (Brisighella, N Italy). Boll. Soc. Paleontol. Italiana, **28**, 265–270.

FLECKER, R. & ELLAM, R.M. (2006) Identifying Late Miocene episodes of connection and isolation in the Mediterranean-Paratethyan realm using Sr isotopes. Sed. Geol., **188–189**, 189–203.

FLECKER, R., de VILLIERS, S. & ELLAM, R.M. (2002) Modelling the effect of evaporation on the salinity–87Sr/86Sr relationship in modern and ancient marginal-marine systems: the Mediterranean Messinian Salinity Crisis. Earth Planet. Sci. Lett., **203**, 221–233.

FOLLOWS, E.J. (1990) Sedirnentology and tectonic setting of Miocene reef and related sediments in Cyprus. PhD Thesis, Edinburgh University, 384 pp.

FOLLOWS, E.J. (1992) Patterns of reef sedimentation and diagenesis in Cyprus. Sed. Geol., **79**, 225–253.

FOLLOWS, E.J., ROBERTSON, A.H.F. & SCOFFIN, T.P. (1996) Tectonic controls on Miocene reefs and related carbonate facies in Cyprus. In: Models for Carbonate Stratigraphy from Miocene Reef Complexes of Mediterranean Regions. SEPM Concepts in Sedimentology and Paleontology (Eds E.K. Franseen, M. Esteban, W.C. Ward & J.-M. Rouchy), 5, pp. 295–325. SEPM (Society for Sedimentary Geology), Tulsa, OK.

GASS, T.M. (1960) The geology and mineral resources of the Dhali area. Geol. Surv. Depart. Cyprus Mem., **4**, 116.

GENNARI, R., IACCARINO, S.M., DI STEFANO, A., STURIALE, G., CIPOLLARI, P., MANZI, V., ROVERI, M. & COSENTINO, D. (2008) The Messinian–Zanclean boundary in the Northern Apennine. Stratigraphy, **5**, 307–322.

GENNARI, R., MANZI, V., ANGELETTI, L., BERTINI, A., BIFFI, U., CEREGATO, A., FARANDA, C., GLIOZZI, E., LUGLI, S., MENICHETTI, E., ROSSO, A., ROVERI, M. & TAVIANI, M. (2013) A shallow water record of the onset of the Messinian salinity crisis in the Adriatic foredeep (Legnagnone section, Northern Apennines). Palaeogeogr. Palaeoclimatol. Palaeoecol., **386**, 145–164.

GLIOZZI, E. & GROSSI, F. (2008) Late Messinian lago-mare ostracod palaeoecology: a correspondence analysis approach. Palaeogeogr. Palaeoclimatol. Palaeoecol., **264**, 288–295.

GUERRA-MERCHAN, A., SERRANO, F., GARCES, M., GOFAS, S., ESU, D., GLIOZZI, E. & GROSSI, F. (2010) Messinian Lago-Mare deposits near the Strait of Gibraltar (Malaga Basin, S Spain). Palaeogeogr. Palaeoclimatol. Palaeoecol., **285**, 264–276.

GVIRTZMAN, Z., RESHEF, M., BUCH-LEVIATAN, O. & BEN-AVRAHAM, B. (2013) Intense salt deformation in the Levant Basin in the middle of the Messinian Salinity Crisis. Earth Planet. Sci. Lett., **379**, 108–119.

HILGEN, F.J. & KRIJGSMAN, W. (1999) Cyclostratigraphy and astrochronology of the Tripoli diatomite formation (pre-evaporite Messinian, Sicily, Italy). Terra Nova, **11**, 16–22.

HILGEN, F.J., KUIPER, K., KRIJGSMAN, W., SNEL, E. & van der LAAN, E. (2007) Astronomical tuning as the basis for high resolution chronostratigraphy: the intricate history of the Messinian Salinity Crisis. Stratigraphy, **4**, 231–238.

HEUBSCHER, C., CARTWRIGHT, J., CYPIONKA, H., de LANGE, G., ROBERTSON, A., SUC, J.P. & URAI, J. (2007) Global look at Salt Giants. EOS, **88**(16), 177–179.

HUGUEN, C., MASCLE, J., CHAUMILLON, E., WOODSIDE, J.M., BENKHELIL, J., KOPF, A. & VOLKONSKAIA, A. (2001) Deformational styles of the Eastern Mediterranean ridge and surroundings, from combined swath-mapping and seismic reflection profiling. Tectonophysics, **343**, 21–47.

KARAKITSIOS, V., ROVERI, M., LUGLI, S., MANZI, V., GENNARI, R., ANTONARAKOU, A., TRIANTAPHYLLOU, M., AGIADI, K. & KONTAKIOTIS, G. (2013) Remarks on the Messinian evaporites of Zakynthos Island (Ionian Sea, Eastern Mediterranean). Bull. Geol. Soc. Greece, XLVII.

KINNAIRD, T.C. & ROBERTSON, A.H.F. (2013) Tectonic and sedimentary response to subduction and incipient continental

collision in southern Cyprus, easternmost Mediterranean region. Geol. Soc. Spec. Publ., **372**, 585–614.

KINNAIRD, T.C., ROBERTSON, A.H.F. & MORRIS, A. (2011) Timing of uplift of the Troodos Massif (Cyprus) constrained by sedimentary and magnetic polarity evidence. J. Geol. Soc. London, **168**, 457–470.

KOUWENHOVEN, T.J., MORIGI, C., NEGRI, A., GIUNTA, S., KRIJGSMAN, W. & ROUCHY, J.-M. (2006) Paleoenvironmental evolution of the eastern Mediterranean during the Messinian: constraints from integrated microfossil data of the Pissouri Basin (Cyprus). Mar. Micropaleontol., **60**, 17–44.

KRIJGSMAN, W., HILGEN, F.J., RAFFI, I., SIERRO, F.J. & WILSON, D.S. (1999) Chronology, causes, and progression of the Messinian salinity crisis. Nature, **400**, 652–655.

KRIJGSMAN, W., BLANC-VALLERON, M.M., FLECKER, R., HILGEN, F.J., KOUWENHOVEN, T.J., ORSZAG-SPERBER, F. & ROUCHY, J.M. (2002) The onset of the Messinian salinity crisis in the eastern Mediterranean (Pissouri basin, Cyprus). Earth Planet. Sci. Lett., **194**(3–4), 299–310.

KRIJGSMAN, W., GABOARDI, S., HILGEN, F.J., IACCARINO, S., de KAENEL, E. & van der LAAN, E. (2004) Revised astrochronology for the Ain el Beida section (Atlantic Morocco): no glacioeustatic control for the onset of the Messinian Salinity Crisis. Stratigraphy, **1**, 87–101.

Le PICHON, X., LALLEMANT, S.J., CHAMOT-ROOKE, N., LEMEUR, D. & PASCAL, G. (2002) The Mediterranean Ridge backstop and the Hellenic nappes. Mar. Geol., **186**, 111–125.

LOFI, J., GORINI, C., BERN_E, S., CLAUZON, G., TADEU DOS REIS, A., RYAN, W.B.F. & STECKLER,M. (2005) Erosional processes and paleo-environmental changes in the Western Gulf of Lions (SW France) during the Messinian Salinity Crisis. Mar. Geol., **217**, 1–30.

LOFI, J., D_EVERCH_ERE, J., GAULLIER, V., GILLET, H., GORINI, C., GUENNOC, P., LONCKE, L., MAILLARD, A., SAGE, F. & THINON, I. (2011) Seismic atlas of the "Messinian Salinity Crisis" markers in the Mediterranean and Black seas. Commission for the Geological Map of the World and Memoires de la Soci_Et_E G_Eologique de France, Nouvelle S_Erie, , p. 72.

LORD, A.R., HARRISON, R.W., BOUDAGHER-FADEL, M., STONE, B.D. & VAROL, O. (2009) Miocene mass-transport sediments, Troodos Massif, Cyprus. Proc. Geol. Assoc., **120**, 133–138.

LOWE, D.R. & GUY, M. (2000) Slurry-flow deposits in the Britannia Formation (Lower Cretaceous), North Sea: a new perspective on the turbidity current and debris flow problem. Sedimentology, **47**, 31–70.

LOZAR, F., VIOLANTI, D., DELA PIERRE, F., BERNARDI, E., CAVAGNA, S., CLARI, P., IRACE, A., MARTINETTO, E. & TRENKWALDER, S. (2010) Calcareous nannofossils and foraminifers herald the Messinian Salinity Crisis: the Pollenzo section (Alba, Cuneo; NW Italy). Geobios, **43**, 21–32.

LUGLI, S., SCHREIBER, B.C. & TRIBERTI, B. (1999) Giant polygons in the Realmontemine (Agrigento, Sicily): evidence for the desiccation of a Messinian halite basin. J. Sediment. Res., **69**, 764–771.

LUGLI, S., MANZI, V., ROVERI, M. & SCHREIBER, B.C. (2010) The Primary Lower Gypsum in the Mediterranean: a new facies interpretation for the first stage of the Messinian salinity crisis. Palaeogeogr. Palaeoclimatol. Palaeoecol., **297**, 83–99.

LUGLI, S., GENNARI, R., GVIRTZMAN, Z., MANZI, V., ROVERI, M. & SCHREIBER, B.C. (2013) Evidence of clastic evaporites in the canyons of the Levant Basin (Israel): implications for the Messinian Salinity Crisis. J. Sediment. Res., **83**, 942–954.

MAILLARD, A., HUEBSHER, C., BENKHELIL, J. & TAHCHI, E. (2010) Deformed Messinian markers in the Cyprus Arc: tectonic and/or Messinian salinity crisis indicators? Basin Res., **23**–2, 146–170.

MANZI, V., LUGLI, S., RICCI LUCCHI, F. & ROVERI, M. (2005) Deep-water clastic evaporites deposition in the Messinian

Adriatic foredeep (northern Apennines, Italy): did the Mediterranean ever dry out? Sedimentology, 52, 875–902.

MANZI, V., ROVERI, M., GENNARI, R., BERTINI, A., BIFFI, U., GIUNTA, S., IACCARINO, S.M., LANCI, L., LUGLI, S., NEGRI, A., RIVA, A., ROSSI, M.E. & TAVIANI, M. (2007) The deep-water counterpart of the Messinian Lower Evaporites in the Apennine foredeep: the Fanantello section (Northern Apennines, Italy). Palaeogeogr. Palaeoclimatol. Palaeoecol., 251, 470–499.

MANZI, V., LUGLI, S., ROVERI, M. & SCHREIBER, B.C. (2009) A new facies model for the Upper Gypsum of Sicily (Italy): chronological and palaeoenvironmental constraits for the Messinian salinity crisis in the Mediterranean. Sedimentology, 56, 1937–1960.

MANZI, V., LUGLI, S., ROVERI, M., SCHREIBER, B.C. & GENNARI, R. (2011) The Messinian "Calcare di Base" (Sicily, Italy) revisited. GSA Bull., 123(1–2), 347–370.

MANZI, V., GENNARI, R., LUGLI, S., ROVERI, M., SCAFETTA, N. & SCHREIBER, B.C. (2012) High-frequency cyclicity in the Mediterranean Messinian evaporites: evidence for solar-lunar climate forcing. J. Sediment. Res., 82, 991–1005.

MANZI, V., GENNARI, R., HILGEN, F., KRIJGSMAN, W., LUGLI, S., ROVERI, M. & SIERRO, F.J. (2013) Age refinement of the Messinian salinity crisis onset in the Mediterranean. Terra Nova, 25, 315–322.

MASCLE, J. & CHAUMILLON, E. (1998) An overview of Mediterranean Ridge collisional accretionary complex as deduced from multichannel seismic data. Geo-Mar. Lett., 18, 81–89.

MCCALLUM, J.E. & ROBERTSON, A.H.F. (1995) Sedimentology of two fan delta systems in the Pliocene-Pleistocene of the Mesaoria Basin, Cyprus. Sed. Geol., 98, 215–244.

MCCAY, G.A. & ROBERTSON, A.H.F. (2013) Upper Miocene-Pleistocene deformation of the Girne (Kyrenia) Range and Dar Dere (Ovgos) lineaments, northern Cyprus: role in collision and tectonic escape in the easternmost Mediterranean region. Geol. Soc. Spec. Publ., 372, 421–445.

MERLE, D., LAURIAT-RAGE, A., GAUDANT, J., PESTREA, S., COURME-RAULT, M.D., ZORN, I., BLANC-VALLERON, M.-M., ROUCHY, J.M., ORSZAG-SPERBER, F. & KRIJGSMAN, W. (2002) Les pal_Eopeuplements marins du Messinien pr_E-_Evaporitique de Pissouri (Chypre, M_Editerran_Ee orientale): aspects pal_Eo_Ecologiques de la crise de salinit_E messinienne. Geodiversitas, 24, 669–689.

MORIGI, C., NEGRI, A., GIUNTA, S., KOUWENHOVEN, T., KRIJGSMAN, W., BLANC-VALLERON, M.-M., ORSZAG-SPERBER, F. & ROUCHY, J.-M. (2007) Integrated quantitative biostratigraphy of the latest Tortonian-early Messinian Pissouri section (Cyprus): an evaluation of calcareous plankton bioevents. Geobios, 40/3, 267–279.

OMODEO-SAL_E, S., GENNARI, R., LUGLI, S.,MANZI, V.&ROVERI, M. (2012) Tectonic and climatic control on the Late Messinian sedimentary evolution of the Nijar Basin (Betic Cordillera, Southern Spain). Basin Res., 24, 314–337.

ORSZAG-SPERBER, F., CARUSO, A., BLANC-VALLERON, M.M., MERLE, D. & ROUCHY, J.M. (2009) The onset of the Messinian salinity crisis: insights from Cyprus sections. Sed. Geol., 217, 52–64.

PANTAZIS, T.M. (1967) The geology and mineral resources of the Pharmakas – Kalavasos area. Geol. Surv. Depart. Cyprus Mem., 8, 190.

PAYNE, A.S. & ROBERTSON, A.H.F. (1995) Neogene supra-subduction zone extension in the Polis graben system, west Cyprus. J. Geol. Soc. London, 152, 613–628.

ROBERTSON, A.H.F. (1976) Pelagic chalks and calciturbidites from the lower Tertiary of the Troodos Massif, Cyprus. J. Sediment. Res., 46, 1007–1016.

ROBERTSON, A.H.F. (1998) Late Miocene paleoenvironments and tectonic setting of the southern margin of Cyprus and the

Eratosthenes seamount. Proc. Ocean Drill. Prog. Sci. Results, 160, 453–464.

ROBERTSON, A.H.F., EATON, S., FOLLOWS, E.J. & PAYNE, A.S. (1995) Depositional processes and basin analysis of Messinian evaporites in Cyprus. Terra Nova, 7, 233–253.

ROUCHY, J.M. (1982) La crise evaporitique messinienne de Mediterranee: nouvelles propositions pour une interpretation genetique. Thesis, Mem, p. 280. Mus. Natn. Hist. Nat, Paris.

ROUCHY, J.M. & CARUSO, A. (2006) The Messinian salinity crisis in the Mediterranean basin: a reassessment of the data and an integrated scenario. Sed. Geol., 188, 35–67.

ROUCHY, J.M., ORSZAG-SPERBER, F., BLANC-VALLERON, M.M., PIERRE, C., RIVI_ERE, M., COMBOURIEU-NEBOUT, N. & PANAYIDES, I. (2001) Paleoenvironmental changes at the Messinian-Pliocene boundary in the eastern Mediterranean: southern Cyprus basins. Sed. Geol., 145, 93–117.

ROVERI, M. & MANZI, V. (2006) The Messinian salinity crisis: looking for a new paradigm? Palaeogeogr. Palaeoclimatol. Palaeoecol., 238, 386–398.

ROVERI, M., MANZI, V., BASSETTI, M.A., MERINI, M. & RICCI LUCCHI, F. (1998) Stratigraphy of the Messinian post-evaporitic stage in eastern-Romagna (northern Apennines, Italy). Giorn. Geol., 60, 119–142.

ROVERI, M., BASSETTI, M.A. & RICCI LUCCHI, F. (2001) The Mediterranean Messinian Salinity Crisis: an Apennine foredeep perspective. Sediment. Geol., 140, 201–214.

ROVERI, M., MANZI, V., RICCI LUCCHI, F. & ROGLEDI, S. (2003) Sedimentary and tectonic evolution of the Vena del Gesso basin (Northern Apennines, Italy): implications for the onset of the Messinian salinity crisis. Geol. Soc. Am. Bull., 115, 387–405.

ROVERI, M., LUGLI, S., MANZI, V. & SCHREIBER, B.C. (2008a) The Messinian Sicilian stratigraphy revisited: toward a new scenario for the Messinian salinity crisis. Terra Nova, 20, 483–488.

ROVERI, M., LUGLI, S., MANZI, V. & SCHREIBER, B.C. (2008b) The Messinian salinity crisis: a sequence –stratigraphic approach. Geoacta Spec. Publ., 1, 169–190.

ROVERI, M., BERTINI, A., COSENTINO, D., DI STEFANO, A., GENNARI, R., GLIOZZI, E., GROSSI, F., IACCARINO, S.M., LUGLI, S., MANZI, V. & TAVIANI, M. (2008c) A high-resolution stratigraphic framework for the latest Messinian events in the Mediterranean area. Stratigraphy, 5, 323–342.

ROVERI, M., FLECKER, R., KRIJGSMAN, W., LOFI, J., LUGLI, S., MANZI, V., SIERRO, F.J., BERTINI, A., CAMERLENGHI, A., DE LANGE, G.J., GOVERS, R., HILGEN, F.J., HUBSCHER, C., MEIJER, P.T.H. & STOICA, M. (2014a) The Messinian Salinity Crisis: past and future of a great challenge for marine sciences. Mar. Geol., doi: 10.1016/j.margeo.2014.02.002.

ROVERI, M., LUGLI, S., MANZI, V., GENNARI, R. & SCHREIBER, B.C. (2014b) High-resolution strontium isotope stratigraphy of the Messinian deep Mediterranean basins: implications for marginal to central basins correlation. Mar. Geol., 349, 113–125.

ROVERI, M., MANZI, V., BERGAMASCO, A., FALCIERI, F., GENNARI, R. & LUGLI, S. (2014c) Dense shelf water cascading and Messinian canyons: a new scenario for the Mediterranean salinity crisis. Am. J. Sci., 314, 751–784.

SIERRO, F.J., KRIJGSMAN, W., HILGEN, F.J. & FLORES, J.A. (2001) The Abad composite (SE Spain): a Mediterranean reference section for the Messinian and the Astronomical Polarity Time Scale (APTS). Palaeogeogr. Palaeoclimatol. Palaeoecol., 168, 143–172.

STOW, D.A.V., BRAAKENBURG, N.E. & XENOPHONTOS, C. (1995) The Pissouri Basin fan-delta complex, southwestern Cyprus. Sed. Geol., 98, 245–262.

STURANI, C. (1976) Messinian facies in the Piedmont basin. Mem. Soc. Geol. Ital., 16, 11–25.

TAVIANI, M., REMIA, A., ESU, D. & SAMI, M. (2007) Messinian Lago-Mare mollusc fauna from the Gorgona Island slope, Tyrrhenian Sea. Geobios, 40, 351–358.

Ten VEEN, J.H., WOODSIDE, M., ZITTER, T.A.C., DUMONT, J.F., MASCLE, J. & VOLKONSKAIA, A. (2004) Neotectonic evolution of the Anaximander Mountains at the junction of the Hellenic and Cyprus Arcs. Tectonophysics, 391, 35–65.

Van COUVERING, J.A., CASTRADORI, D., CITA, M.B., HILGEN, F.J. & RIO, D. (2000) The base of the Zanclean Stage and of the Pliocene Series. Episodes, 23, 179–187.

Van der LAAN, E., SNEL, E., De KAENEL, E., HILGEN, F.J. & KRIJGSMAN, W. (2006) No major deglaciation across the Miocene-Pliocene boundary: integrated stratigraphy and astronomical tuning of the Loulja sections (Bou Regreg area, NW Morocco). Paleoceanography, 21, PA3011.

Figure captions

Fig. 1. The CIESM (2008)-derived stratigraphic framework (simplified after Manzi et al., 2013) highlighting the three stages of the Messinian salinity crisis and their associated evaporate units and key-surfaces. Evaporite units: PLG (Primary Lower Gypsum), RLG (Resedimented Lower Gypsum), UG (Upper Gypsum). Key surfaces (from the bottom): (1) onset of the Messinian salinity crisis (5.971 Ma; Manzi et al., 2013), (2) Messinian erosional surface (MES; 5.60 Ma; Lofi et al., 2005; Roveri & Manzi, 2006); (3) base of the Upper Gypsum/top of the Halite unit (5.53 Ma; Van der Laan et al., 2006; Hilgen et al., 2007; Manzi et al., 2009); (4) base of the p-ev2 unit (Roveri et al., 1998, 2001; Roveri & Manzi, 2006); (5) base of the Zanclean (5.33 Ma; Van Couvering et al., 2000).

Fig. 2. (a) Simplified map showing the distribution of the Messinian evaporites in the Eastern Mediterranean and the location of the Cyprus Island. (b) Simplified geological and structural map of the Cyprus area including the main depositional basins and the distribution of the Messinian evaporites on the basis of their facies and thickness. (c) Location of the stratigraphic sections (purple stars) described in the text. PoB, Polemi basin; Pib, Pissouri basin; Psb, Psematismenos/Maroni basin; Mb, Mesaoria basin.

Fig. 3. Main lithostratigraphic units of the Cyprus Island after Robertson et al. (1995). In light cyan the hemipelagic deposits that accumulated in the main Cyprus basins during the Late Cretaceous to the Late Miocene interval (Lefkara and Pakhna Formations); in darker cyan the main shallow water reefal units deposited locally on top the main uplifting structural highs of the Cyprus orogen; in light magenta the Kalavasos Formation including all the deposits accumulated during the Messinian salinity crisis.

Fig. 4. Synthetic stratigraphic section of the Messinian deposits in the Cyprus Island by Orszag-Sperber et al. (2009) modified to highlight the evaporite units (light magenta). Added, to the right of the original figure, is the new interpretation presented in this paper. pre-MSC, pre Messinian salinity crisis deposits; RLG, Resedimented Lower Gypsum; UG, Upper Gypsum; MES, Messinian erosional surface.

Fig. 5. Location and general view of the Tokhni sections. (a) Google Earth satellite view of the area 1 km south to the Tokhni Village with the locations of the measured sections (To-0, To-1, To-2, To-3) and the main lithostratigraphic units of the Pakhna Formation (PK-A$_1$, PK-A$_2$, PK-A$_3$, PK-B; see detailed description in the text). The first carbonate bed marking the base of the PK-A$_3$ unit is the yellow line with the ©. M/T is the approximate location of the Tortonian/Messinian Boundary (Orszag-Sperber et al., 2009; this study). It is possible to recognize an E-W elongated anticline with the pre-evaporitic Pakhna Formation in the core and the evaporates of Kalavasos Formation in the flanks. Notice how moving from south to north the Pakhna Formation is progressively cut by the erosional surface (red line) marking the base of the Messinian evaporites, here interpreted as the Messinian erosional surface (MES). (b) Panoramic view of the sector between sections To-0 and To-1 showing the erosional truncation of the upper Pakhna units below the MES. (c) Simplified geological map of the study area with the distribution of the Pakhna Formation (grey), the Kalavasos Formation (light magenta) and its subunits (LU, IU and UU, stand, respectively, for lower, intermediate and upper unit). The location of the sections cited in the text is reported. Yellow circles mark the Tokhni sections (To-0, To-1, To-2, To-3. Yellow stars are for other cited sections: TQ, Tokhni quarry; UG, Upper gypsum section; Ch, outcrop of the Chaotic unit; PQ, Psematismenos quarry. In green the two shot points for pictures (a and b).

Fig. 6. The Tokhni sections used for the reconstruction of the composite section. The subunits of the Pakhna Formation are described in the text. Lithological cycles given by a marl/carbonate couplet are numerated from the younger to the older. Cycle 24 corresponds with the first carbonate bed (©) marking the transition between units PK-A$_2$ and PK-A$_3$.

Fig. 7. The Pakhna Formation. (a) The first carbonate bed (©) marks the passage between subunit PK-A$_2$ and PK-A$_3$. Tokhni section To-1. (b) Detail of the alternation of whitish limestone and red clays characterizing the PK-A$_3$ unit. Tokhni section To-1. (c) Lowermost grainstone layer of unit PK-B; the bed is characterized by a large amount of rip-up clasts of limestone and grainstone. Tokhni section To-2. (d) Composite bed (bed B in Fig. 5) formed by a chaotic brecciated limestone division sandwiched between two laminated grainstone divisions. Tokhni section To-2.

Fig. 8. Microfacies of the Pakhna Fm. limestones. (a) Close up of bed 14 (unit PK-B, Tokni section TO-2). (b) Detail of the upper part of the bed; the laminae are broken apart and reworked by unidirectional currents. (c) Photomicrograph of the lower part of bed 14. Note the laminated structure, given by the alternation of dark and whitish laminae. (d) Detail of C; arrow indicates the filamentous microfossils observed in the micritic laminae. (e) Photomicrograph of the topmost part of bed 16 (unit PK-B, Tokhni section TO-2). Angular intraclasts coated by a rim of laminated micrite (black arrow) are visible. The same rim is developed around skeletal grains (Anellid tube worms, black arrow). (f) SEM image of sample TO4 (Tokhni section To-1) showing an assemblage of coccoliths enclosed by micron-sized calcite crystals.

Fig. 9. Cuspidariid bivalves from marls embedding the 'dismantled' microbialites (the 'M' between carbonate beds B and C in sections To2 + To3 of Fig. 5 mark the exact position) pointing out an outer shelf/upper slope deep marine setting: (a) Cardiomya aff. costellata; (b) Tropidomya aff. abbreviata.

Fig. 10. The Kalavasos Formation. (a) Detail of the composite bed at the base of the Kalavasos Formation in section To-0; the lower chaotic portion including blocks of selenitic gypsum is overlaid by a gypsarenite division with cross to parallel lamination. (b) Fossil remains of Artemia salina on a gypsiltite lamina. Notice the 29 enlargement in the inset. Psematismenos quarry. (c) bird foot prints on a lamina interface. Psematismenos quarry. (d) Gypsarenite graded beds showing normal gradation and bedforms related to

unidirectional currents. x-lam, ripple cross lamination;//-lam, parallel lamination; gar, gypsarenite; cgar, coarsegypsarenite; fgar, fine gypsarenite; m, mud. Psematismenos quarry. (e) fine gypsarenite bed with hummocky cross stratification. Psematismenos quarry.

Fig. 11. Details of the evaporites facies. (a) Photomicrograph of the gypsiltite bearing the Artemia salina shown in Fig. 10b; the rock consists of alternating wavy laminae of slightly reworked wavy gypsum needles cumulates; transmitted light, crossed polars; (b) Alternation of whitish and brownish gypsum cumulates, Tokhni quarry section. (c) Photomicrograph of the previous sample. The rock consists of cumulitic graded laminae of gypsum needles; the lamina at centre contains larger gypsum crystals and appears white on the hand sample, whereas the finer grained laminae appear brownish and contain several discrete events marked by organic matter veneers (not visible at the proposed magnification); transmitted light, crossed polars. (d) Selenite nodules in the laminar gypsum, notice the brownish laminites draping of the whitish nodule. (e) Photomicrograph showing nodules within the laminar gypsum, selenite crystals have random orientation and are grouped in clusters that are draped by the overlaying cumulitic laminar gypsum; transmitted light, crossed polars. (f) Photomicrograph of the mollusk-bearing gypsum laminite. The shells are buried by graded gypsum laminae consisting of granular cumulitic crystals; transmitted light, crossed polars. UG6, Polemi.

Fig. 12. Stratigraphic composite section of the Polemi basin obtained from the outcrops in Kallepya, Lethymbou, Stroumbi and Polemi. The subdivisions adopted in the Orszag-Sperber et al. (2009) (see Fig. 4) are reported. Differently from the previous works, the 'barre jaune' in this paper has been included in the Kalavasos formation because like the overlaying deposits, it contains clasts and blocks of gypsum. Moreover the base of the Kalavasos formation is an angular unconformity corresponding to the Messinian erosional surface (MES) rather than to the onset of the Messinian salinity crisis as previously proposed (Rouchy, 1982; Orszag-Sperber et al., 2009). The location of samples collected for determination of 87Sr/86Sr are numbered from 1 to 6; further details are reported in Table 1.

Fig. 13. Evaporite facies of Lower unit in the Polemi basin. (a) The 'barre jaune' in the Kallepya section. The coarser gypsum clasts, derived from the resedimentation of shallow water bottom-grown selenite, are marked with the letter g. (b) Graded gypsarenite bed sandwiched between two intervals of laminar gypsum. The latter consists of a cm-thick alternation of fine-grained clastic and cumulate gypsum layers (see detail in figure e). Lethymbou. (c) Detail of the base of the gypsarenite bed in Fig. B eroding a gypsum cumulate layer. Lethymbou. (d) Gypsum nodules (ng) related to early growth developed in the upper part of a laminar gypsum (lg) interval. Lethymbou. (e) Detail of a laminar gypsum layer consisting of alternation of withish and brownish laminae. Lethymbou. (f) Detail of a clastic gypsum bed sandwiched between two laminar gypsum beds (lg);x-lam, ripple cross lamination;//-lam, parallel lamination; bps, by-pass surface (i.e. a surface marking an abrupt grainsize break related to the downcurrent bypass of sediment transported by a gravity flow) After the deposition of the clastic gypsum by a gravity flow the chimica precipitation of gypsum started again with the gypsum cumulate. Lethymbou.

Fig. 14. Evaporite facies of Intermediate and Upper units in the Polemi basin (outcrop photographs). (a and b) Onlap of the Upper Gypsum unit (UG) and the underlying Intermediate unit. The lower unit consists of a chaotic interval formed by laminar 'marmara' gypsum. The UG unit consists of an alternation of shallow water primary gypsum deposits (mainly bottom-grown twinned selenite with minor gypsum cumulate and gypsarenite) and shales. Lethymbou. (c) The lowermost three gypsum beds, west of Lethymbou. (d) Large crystals typically found in the UG2 gypsum beds all along the Polemi basin. Lethymbou. (e) Detail of the laminar gypsum of the UG4 layer consisting of a sub-centimetric alternation of small selenite crusts and cumulate gypsum. Lethymbou.

Fig. 15. Fossils findings of the Upper Unit of the Kalavasos Formation. (a) Specimen of the fish skeleton of Aphanius crassicaudus recovered in the shale interval below the second gypsum bed (UG2). Lethymbou. (b and c) Specimen of Limnocardiinae spp recovered in the uppermost gypsum bed (UG-6). Polemi. (d) Lamina interface with mollusc remains. A specimen of Dreissena is 4x enlarged in the inset. Polemi.

Fig. 16. The onset of the Messinian salinity crisis in the Pissouri basin. (a) Alternative age definition of the base of the evaporites in the Pissouri Motorway section, to the right, in comparison with the age model of Krijgsman et al. (2002), to the left: the succession after cycle 4 of Krijgsman et al. (2002) consists of clastic deposits that cannot be easily tuned with the insolation curve; the evaporates overlying the mixed, carbonate and terrigenous, clastic unit are also clastic. (b) Schematic geological map around the Pissouri section. (c) Detail of the composite megabed showing the boundary between the lower chaotic division and the upper stratified and graded division. (d) Clastic carbonate bed in the uppermost portion of the Pakhna Formation with parallel (//-lam), cross (x-lam) and convolute (_-lam) lamination deposited by a gravity flow. (e) The chaotic aspect of the Kalavasos Formation. (f) Detail of gypsrudite including blocks of laminar gypsum (including clastic and cumulate deposits) and clasts and pebbles derived from the dismantlement of primary shallow-water bottom-grown selenite deposits.

Fig. 17. Kato Moni section. (a) Location and schematic geological map of the study area based on Google Earth satellite images; A and B the measured sections. (b) Panoramic view of the Messinian evaporites with indication of cycles and facies reported in the log. (c) Synthetic log. (d) Detailed view of the laminar cumulate facies.

Fig. 18. The stratigraphy of the central Mesaoria basin according to the Xeri borehole (redrawn after Gass, 1960). See Fig. 2 and text description for borehole location.

Fig. 19. The Mediterranean strontium isotope recalibrated after Roveri et al. (2014b) highlighting the new Eastern Mediterranean data and the ones presented in this work.

Fig. 20. N-S schematic geological section along the Southern Cyprus Island across the Troodos Massif. Datum plane base of the Pliocene. Modified from Robertson et al. (1995).

Fig. 21. Tentative correlation and tuning of the stage 3 units of the Messinian salinity crisis of Cyprus, Sicily and Northern Apennines. Original tuning were proposed, respectively, by Manzi et al. (2009), for the Upper Gypsum of Sicily, and by Roveri et al. (2008c), for the evaporite-free units of Northern Apennine.

Fig. 22. Tentative shallow-deep water correlation of the halite unit. (a) onshore Cyprus, Mesaoria Basin, Xeri borehole (redrawn after Gass, 1960; see fig. 18). (b) offshore Cyprus, Larnaca-Latakia basin, synthetic seismic profile of the Messinian salinity crisis units
(from Maillard et al., 2010). (c) offshore Israel, Levant basin, high-resolution seismic profile of the deep halite unit (from Gvirtzman et al., 2013). (d) section locations. Original tuning of halite unit to astronomical and oxygen isotope curves is from Roveri et al. (2014b) (their Fig. S4 of Supplementary File 2).

Table 1. Strontium isotope measured on Cyprus evaporites. The clastic evaporites ascribed to the RLG unit show the typical Lower evaporites signature of $^{87}Sr/^{86}Sr$. Depleted values typical of the Upper Evaporites unit has been obtained from the Upper Gypsum deposits. Samples stratigraphic position is reported in Fig. 12

No	Sample	Unit	$^{87}Sr/^{86}Sr$	Error	Basin	Section	Cycle	LAT	LON	Source
1	PSE-1	RLG	0.708951	0.000020	Maroni/Psematismenos	Psematismenos quarry	–	34°45′33.77″N	33°20′22.89″E	Gypsiltite with brine shrimps (Fig. 10b)
2	PIS-2	RLG	0.708966	0.000020	Pissouri	Pissouri	–	34°40′35.75″N	32°40′3.83″E	Selenite block in the gypsrudite (Fig. 16e)
3	PISS-7	UG	0.708843	0.000020	Pissouri	Pissouri	Local 1st UG	34°40′42.92″N	32°40′15.42″E	Banded selenite
4	TO-1	UG	0.708795	0.000020	Maroni/Psematismenos	Tochni	Local 1st UG	34°46′5.76″N	33°19′31.55″E	Gypsum selenite
5	CY-1-g	UG	0.708847	0.000020	Polemi	Polemi	UG6	34°52′24.28″N	32°30′31.33″E	Gypsum cumulate (Fig. 8)
6	CY-1-m	UG	0.708866	0.000020	Polemi	Polemi	UG6	34°52′24.28″N	32°30′31.33″E	Mollusc shell (Figs 8 and 11)

Table 1
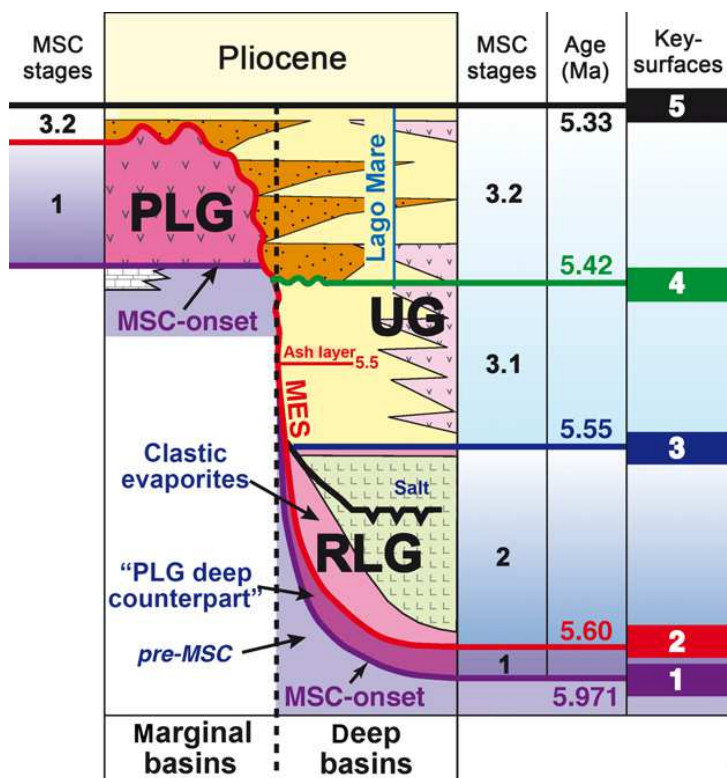
Fig. 1
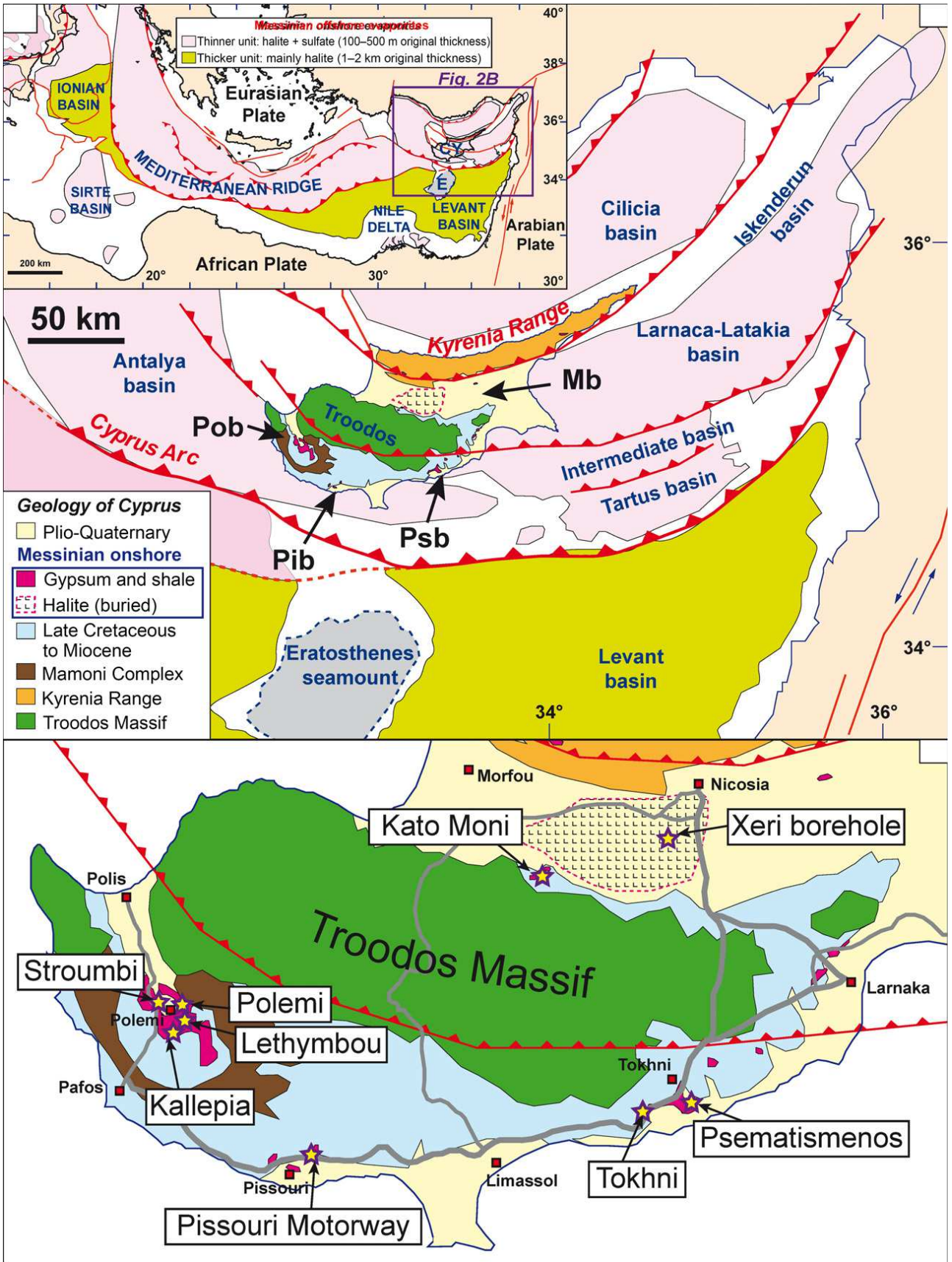
Fig. 2

Age			Formation	Lithology	
Cenozoic	Pleistocene		'Fanglomerate' Apalos	Conglomerate and sandstone	
	Pliocene		Kakkaristra Athalassa	Calcarenite, sandstone, conglomerate	
			Nicosia	Marl, silt, mudstone, sandstone, conglomerate	
	Miocene	Upper	Kalavasos	**Evaporite**	Studied interval
			Koronia member	Reefal and bioclastic limestone	
		Middle	Pakhna	Pelagic chalk, marl, calcarenite, conglomerate	
		Lower	Terra mb.	Reefal and bioclastic limestone	
	Oligocene		Upper Lefkara	Pelagic chalk and marl,	
	Eocene		Middle Lefkara	Massive pelagic chalk	
	Paleocene			Pelagic chalk, replacement chert	
Mesozoic	Maastrichtian		Lower Lefkara	Pelagic chalk	
	Campanian		Kannaviou	Volcaniclastic sandstone, bentonitic clay	
	Turonian		Perapedhi	Umber and radiolarite	
After Robertson et al., 1995			B A S	E M E N T	

Fig. 3
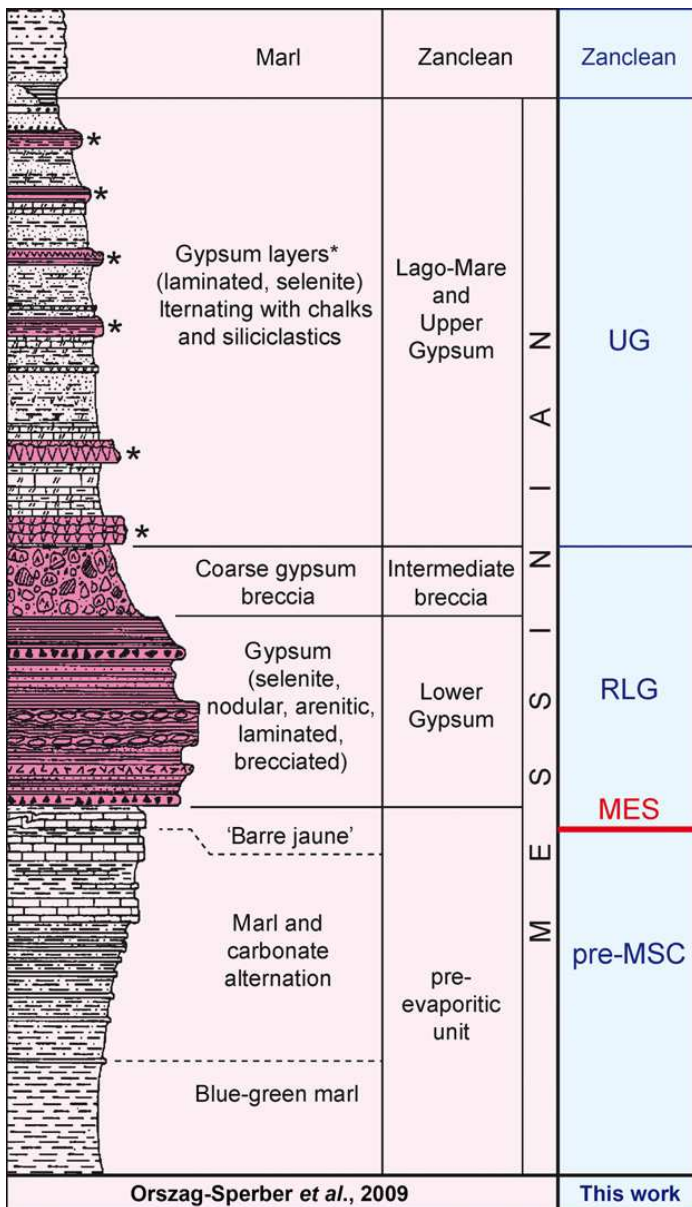
Fig. 4

Fig.5

Fig.6

Fig.7

Fig.8

Fig. 9

Gypsarenite

Chaotic

10 cm

5 mm

2X

1 cm

fgar

cgar

x-lam

m

//-lam

cgar

x-lam

m

gar

gar

//-lam

5 cm

5 cm

Fig.10

Fig. 11

Fig. 12

g   g

g   g

5 cm

Laminar gypsum

Gypsarenite

Laminar gypsum

50 cm

Gypsarenite

Gypsum cumulate

1 cm

lg

x-lam

//-lam

//-lam

//-lam

//-lam

bps

//-lam

lg

Fine gypsarenite

Medium gypsarenite

Coarse gypsarenite

Gypsrudite

15 cm

ng

lg

5 cm

1 cm
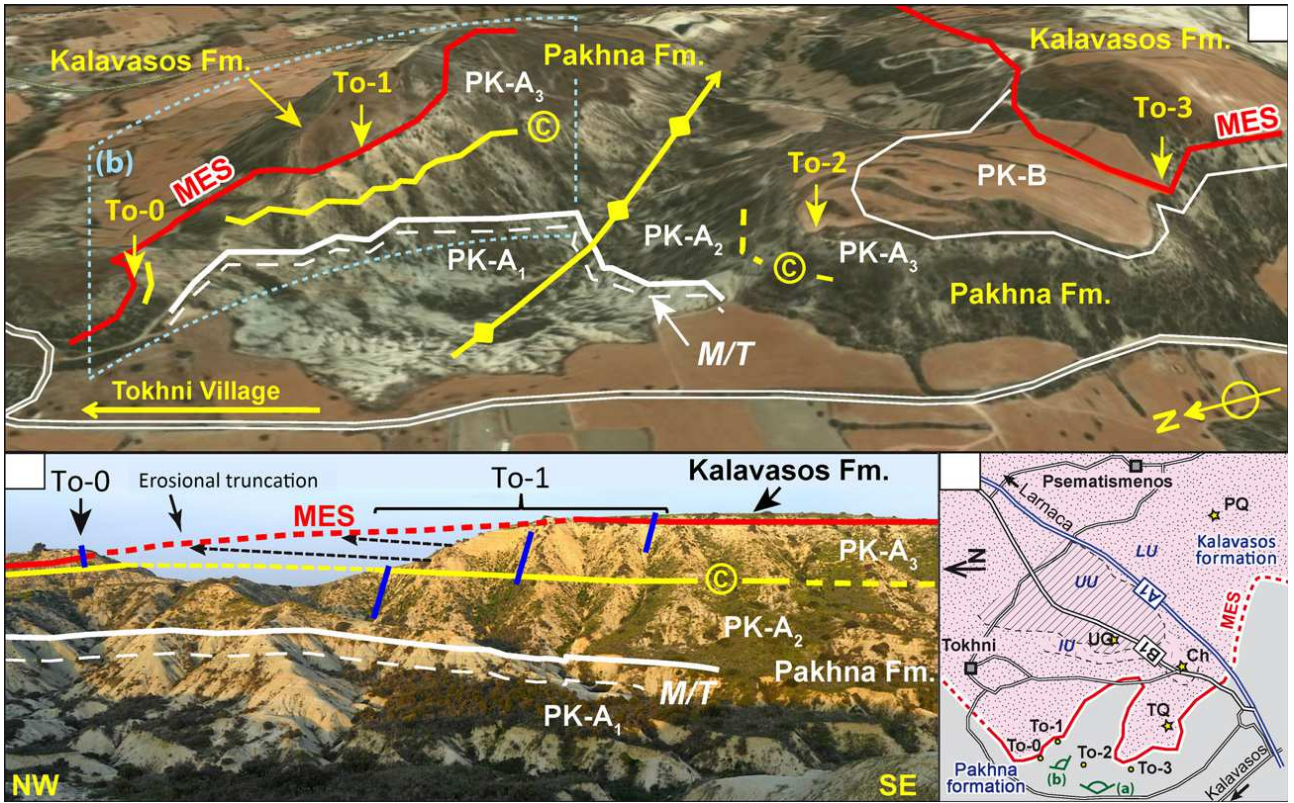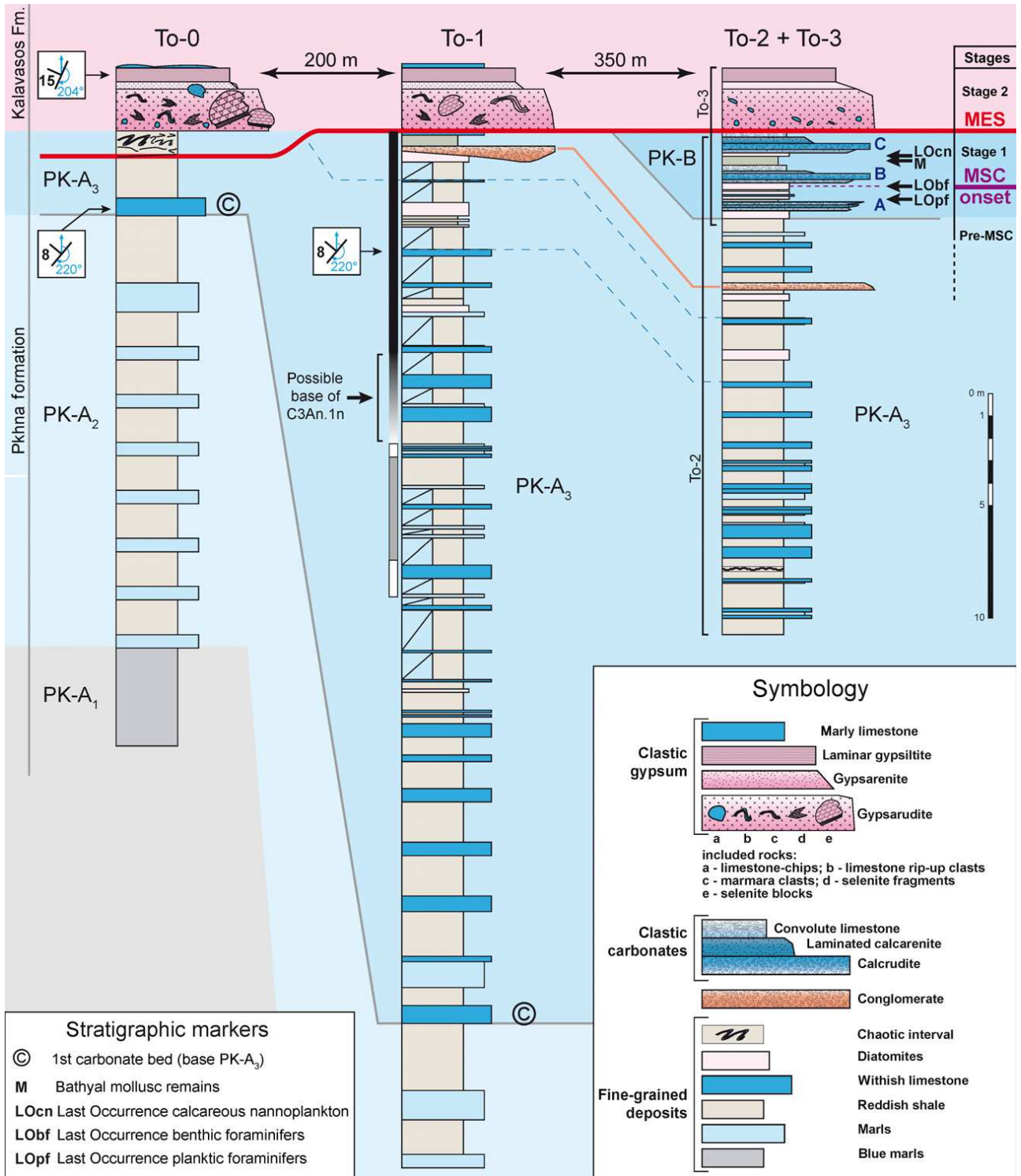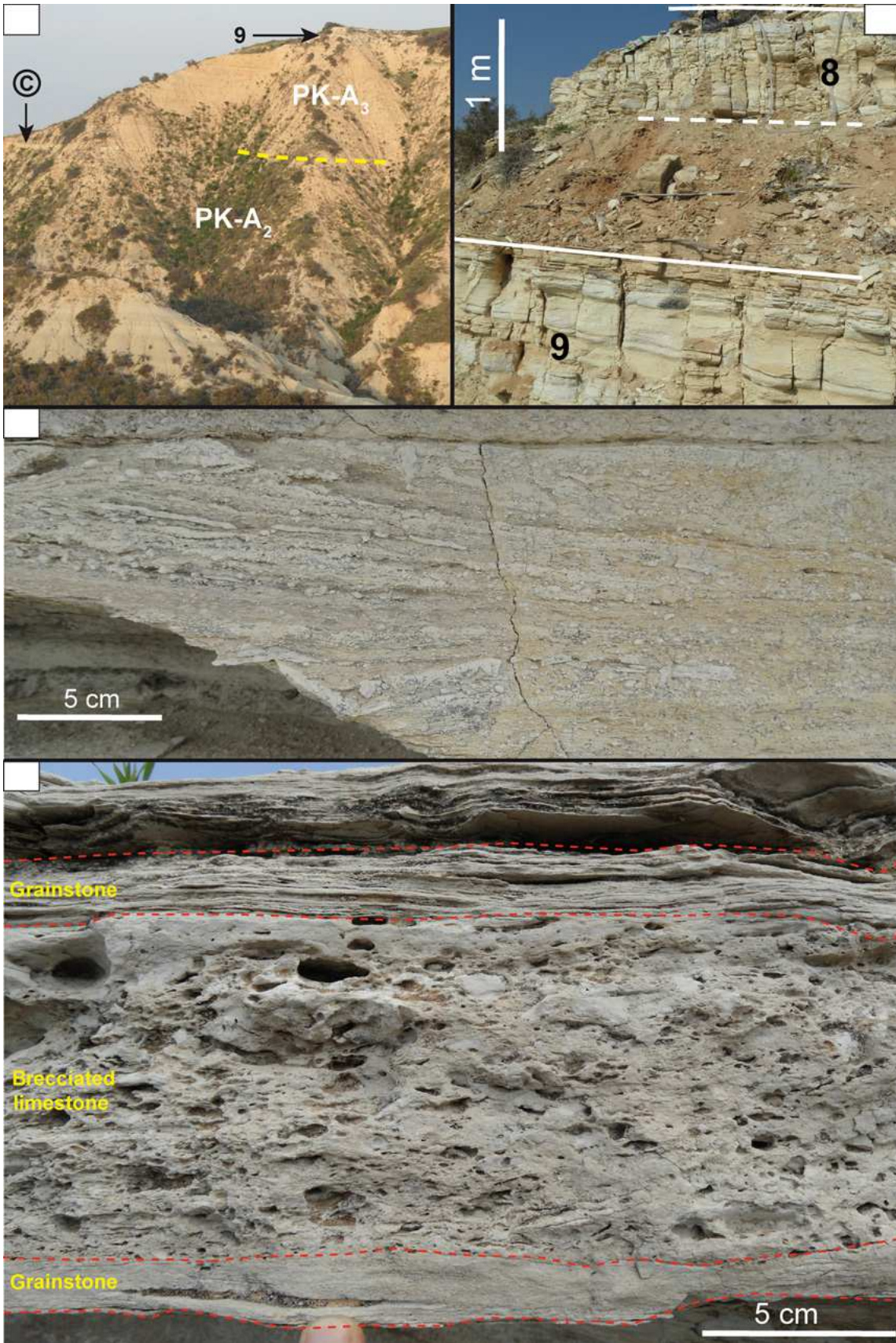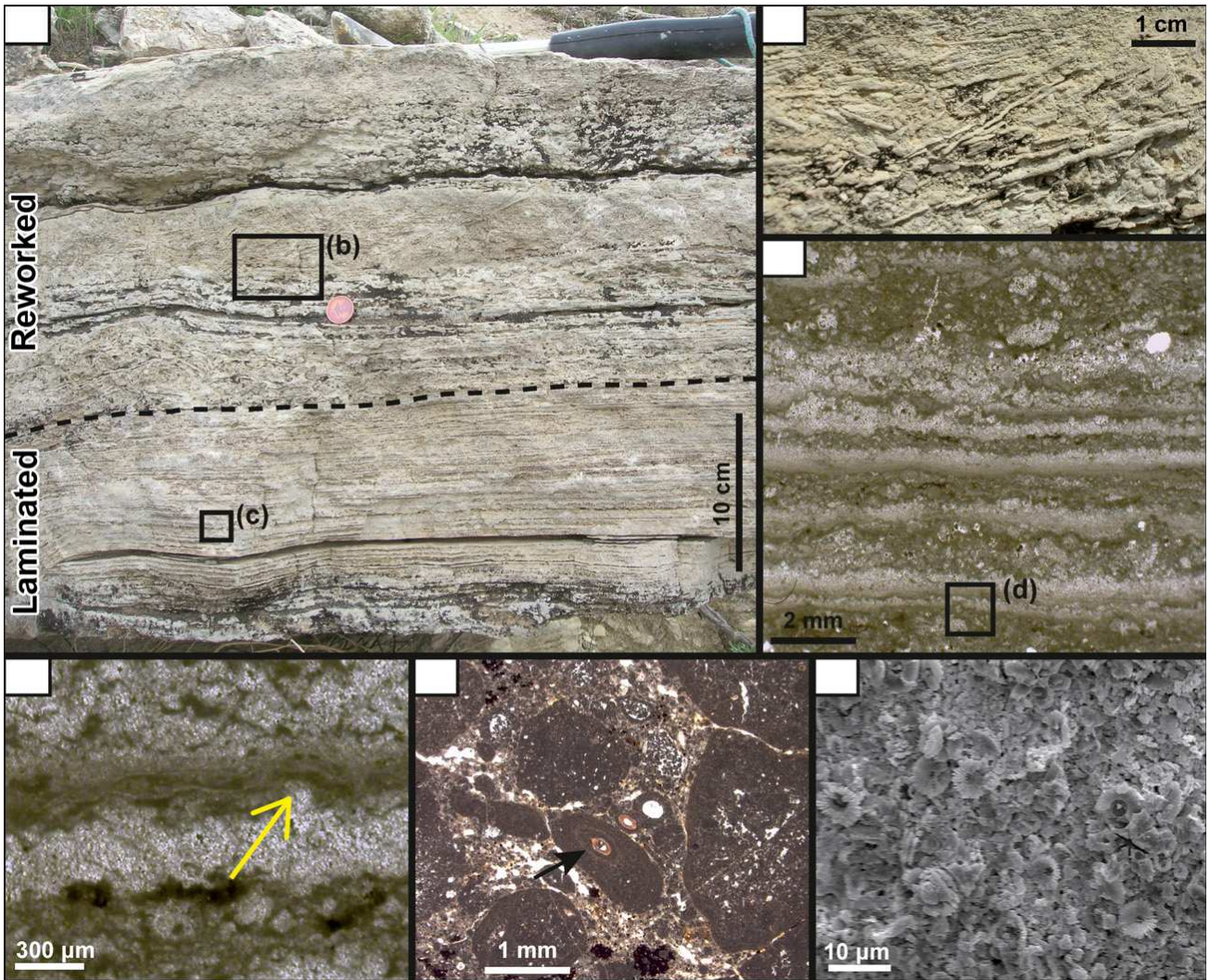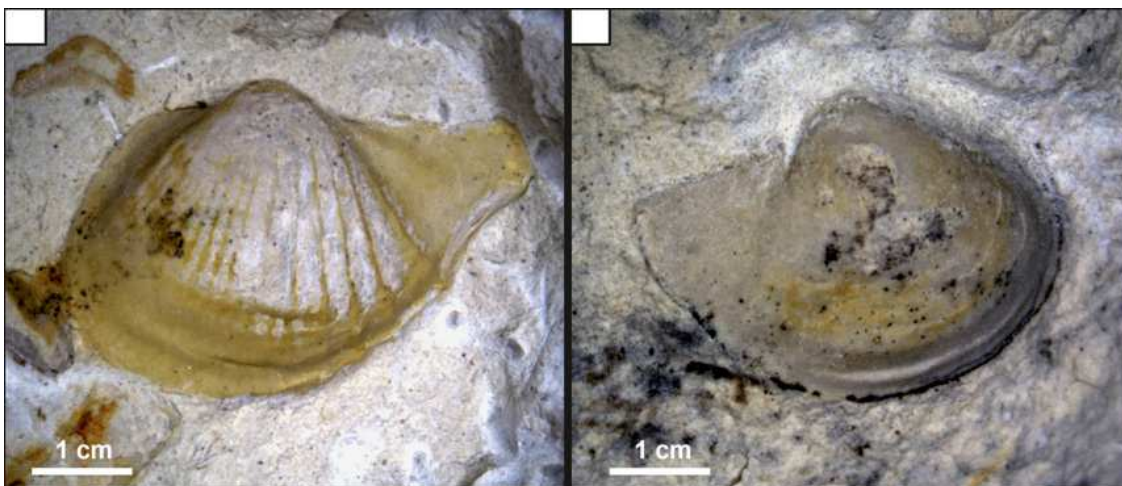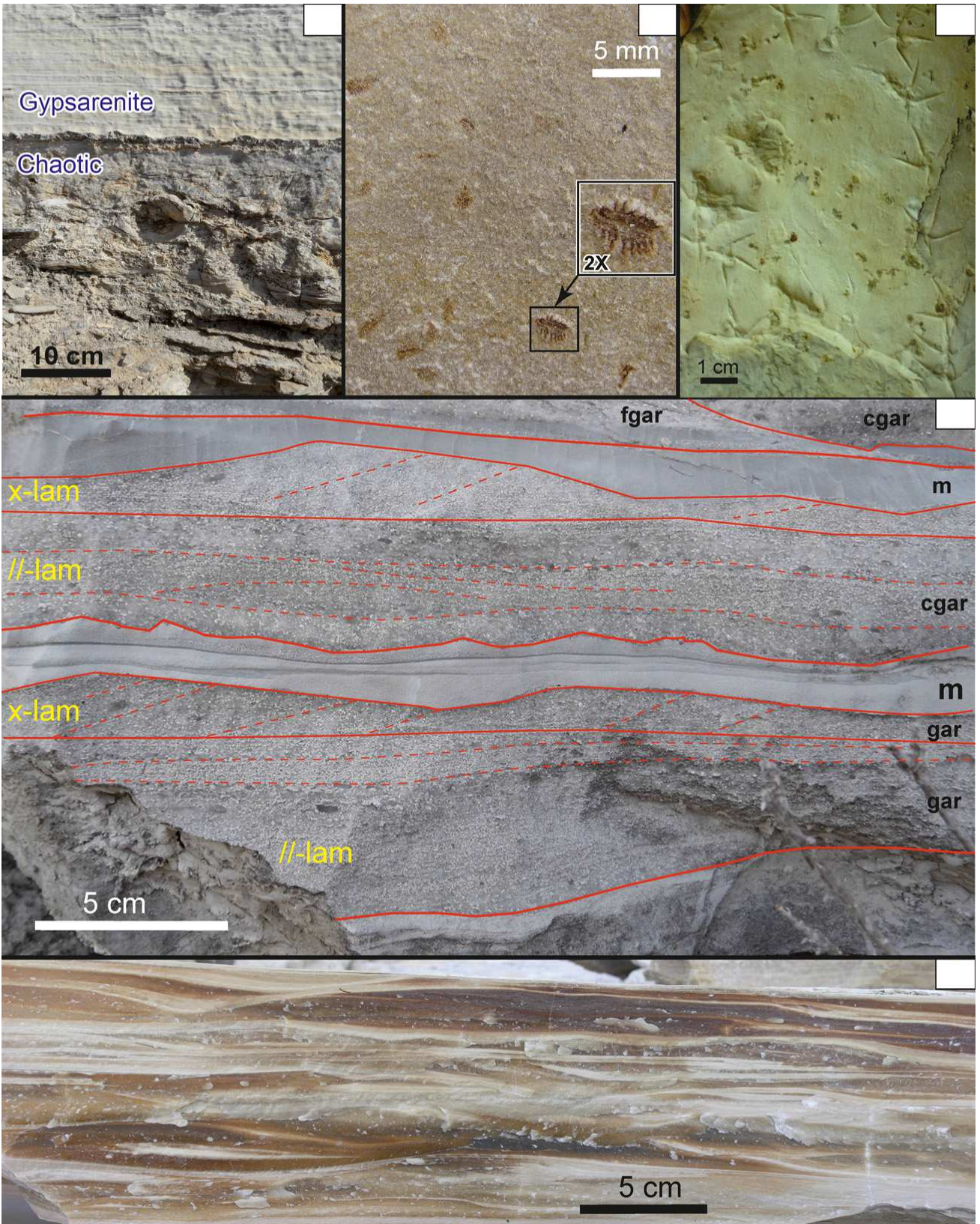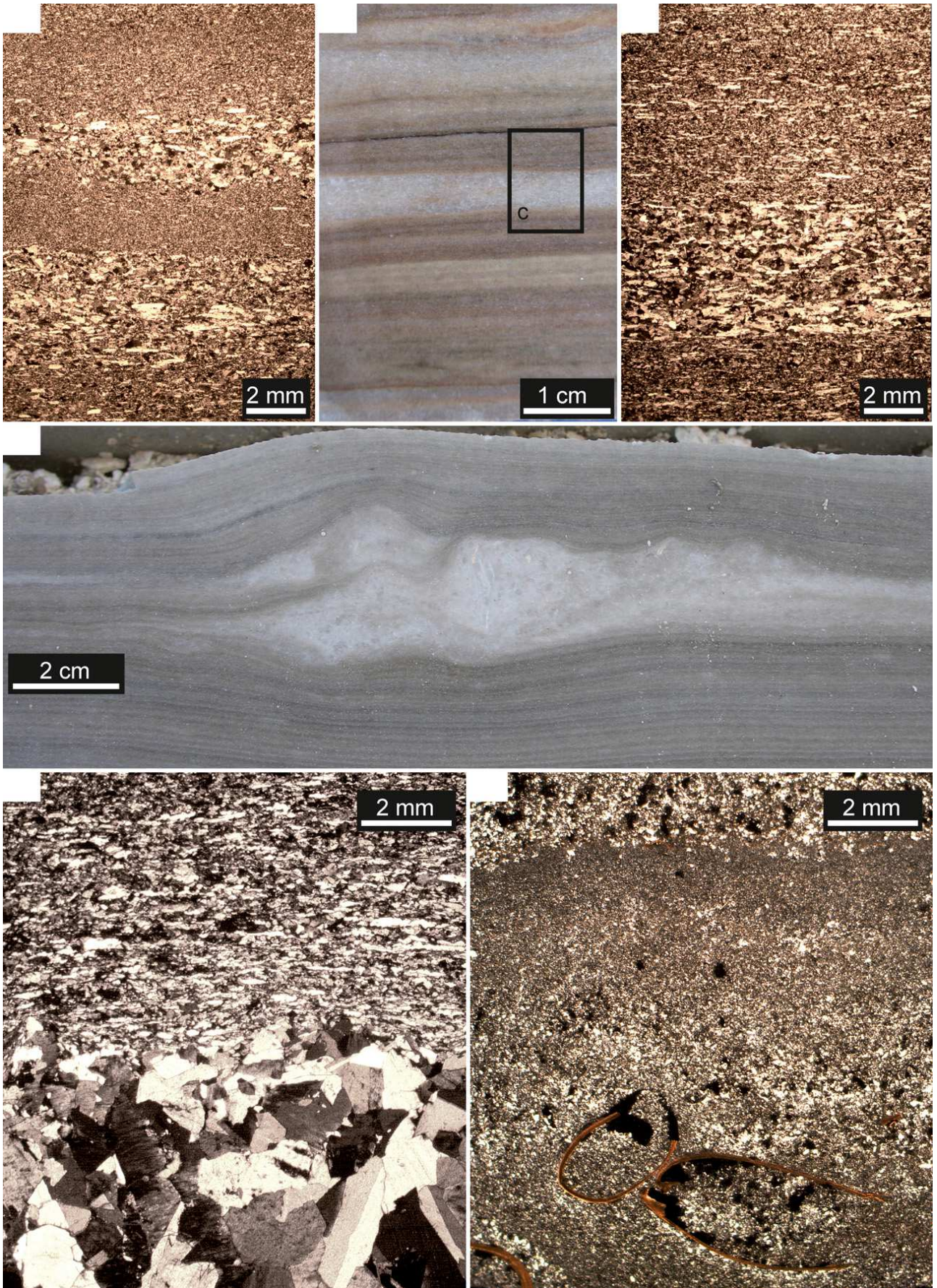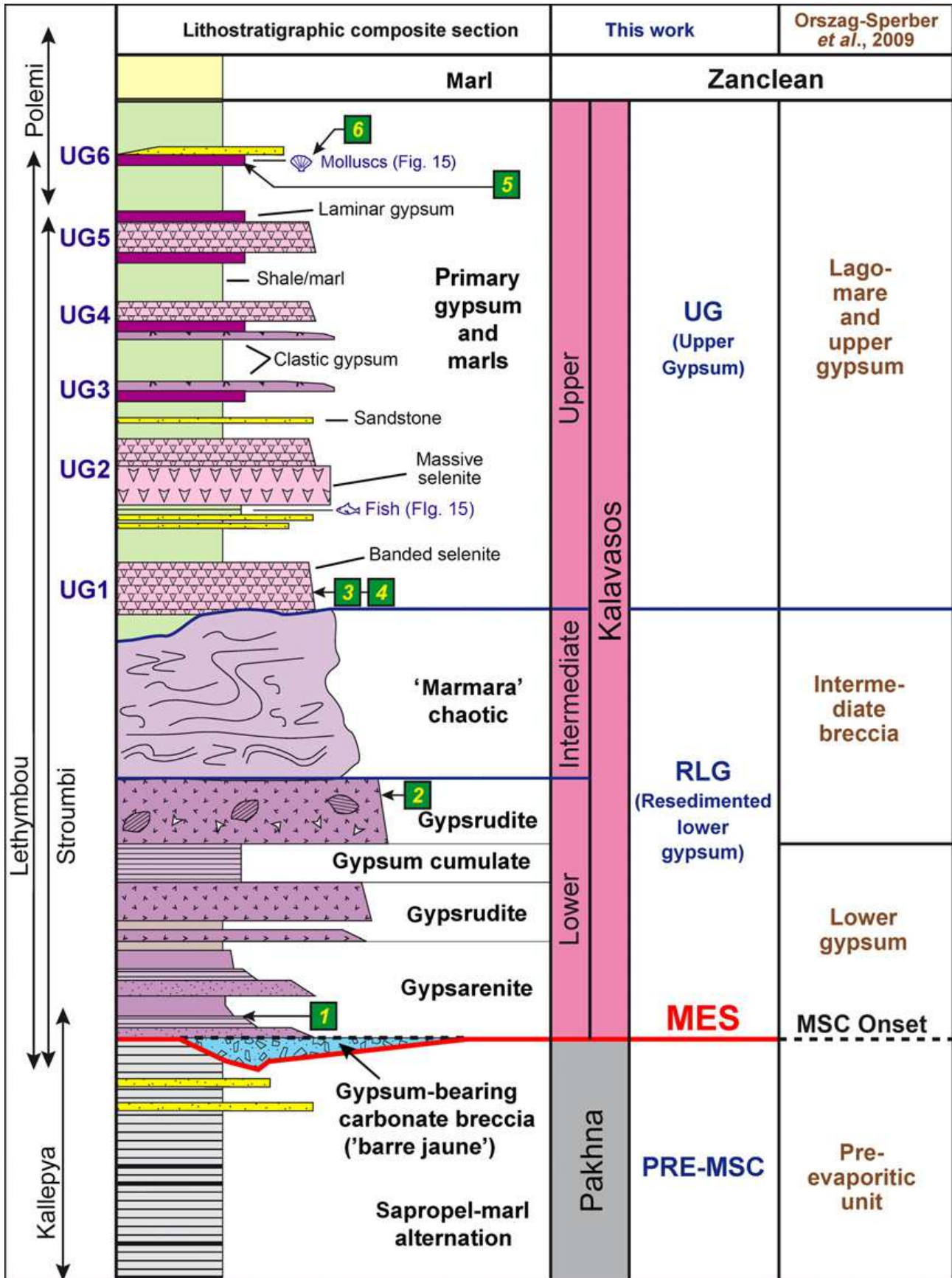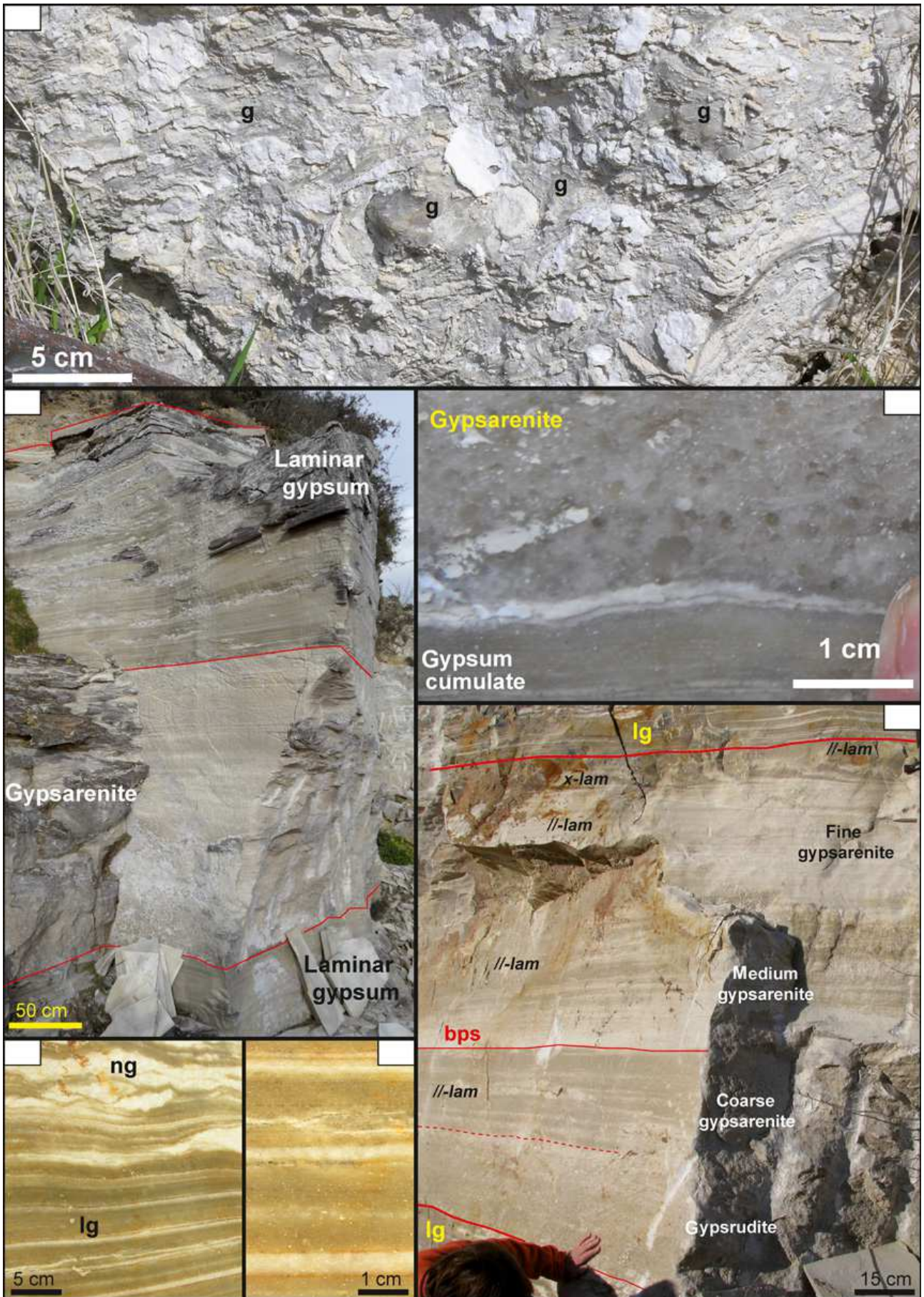
Fig. 13
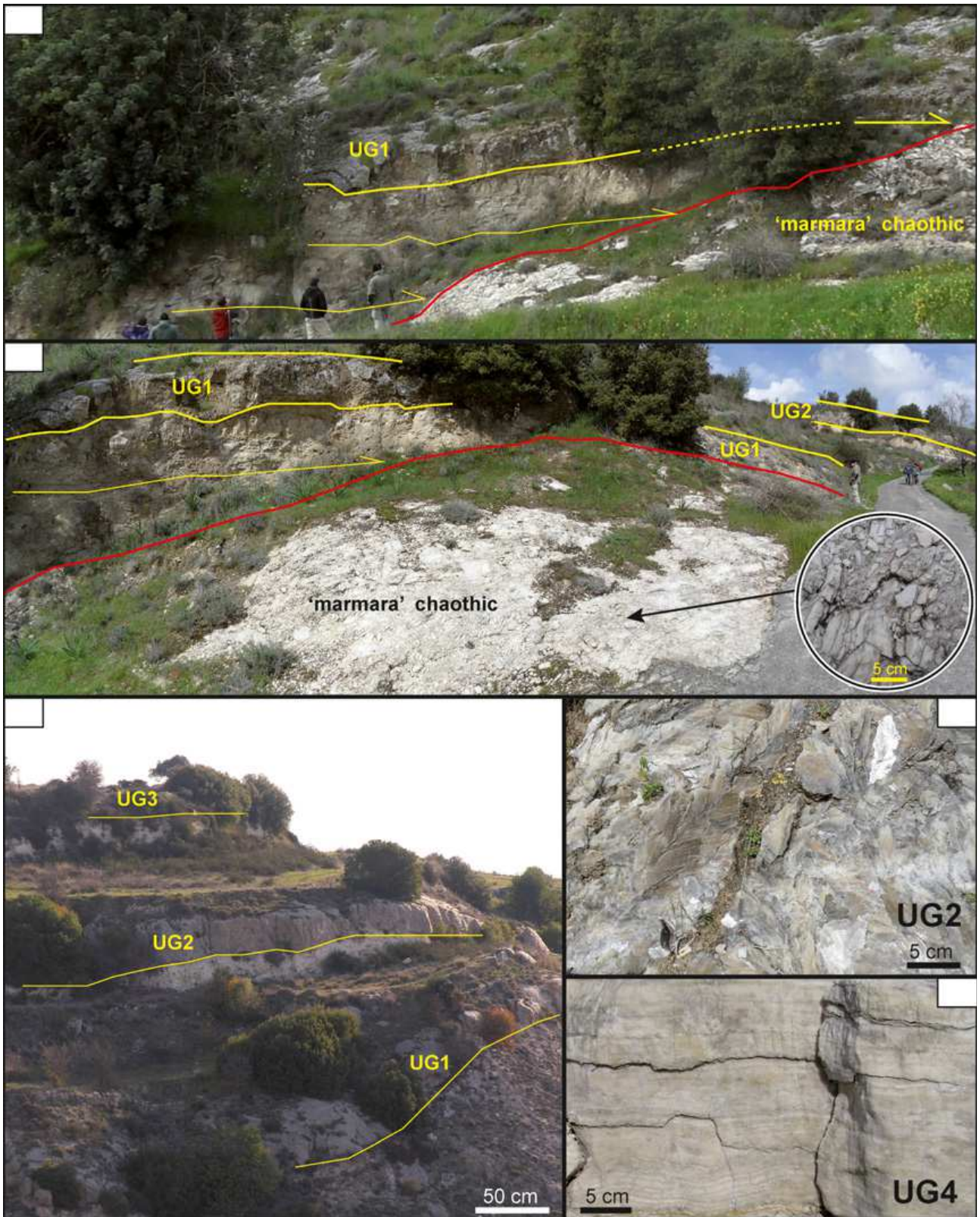
Fig. 14
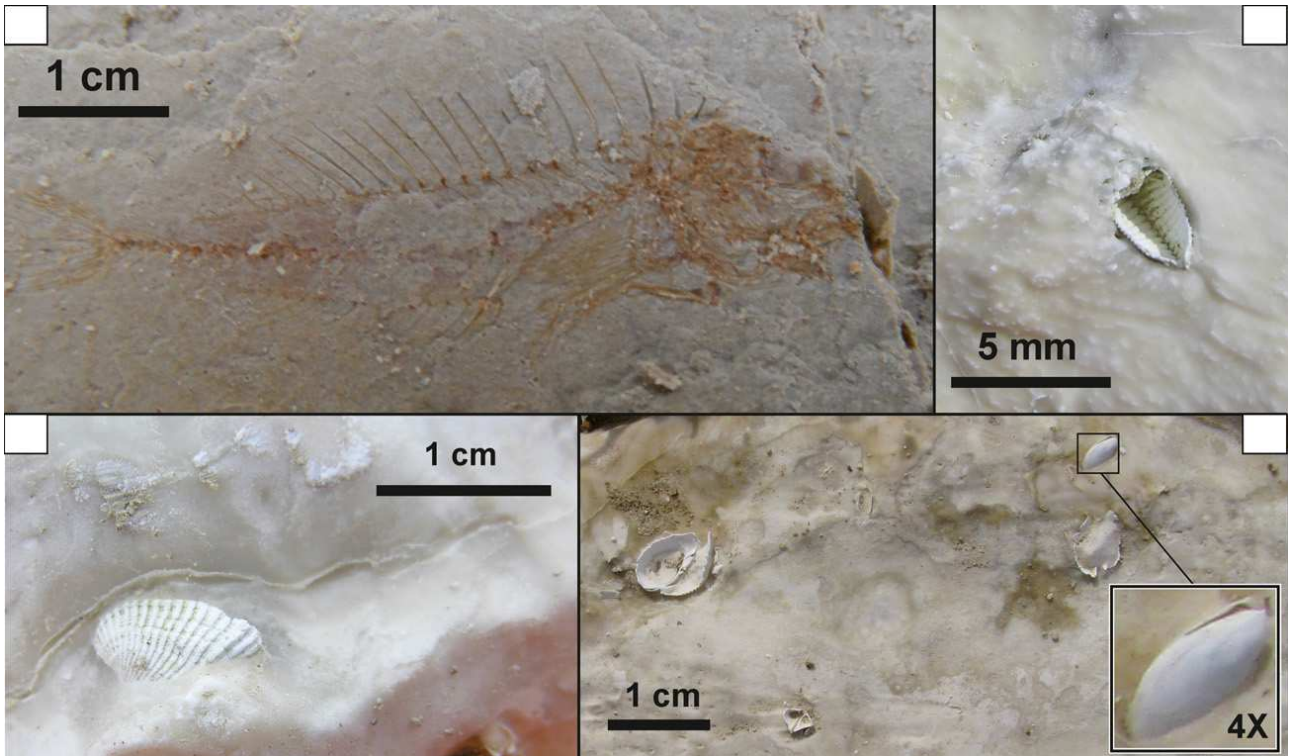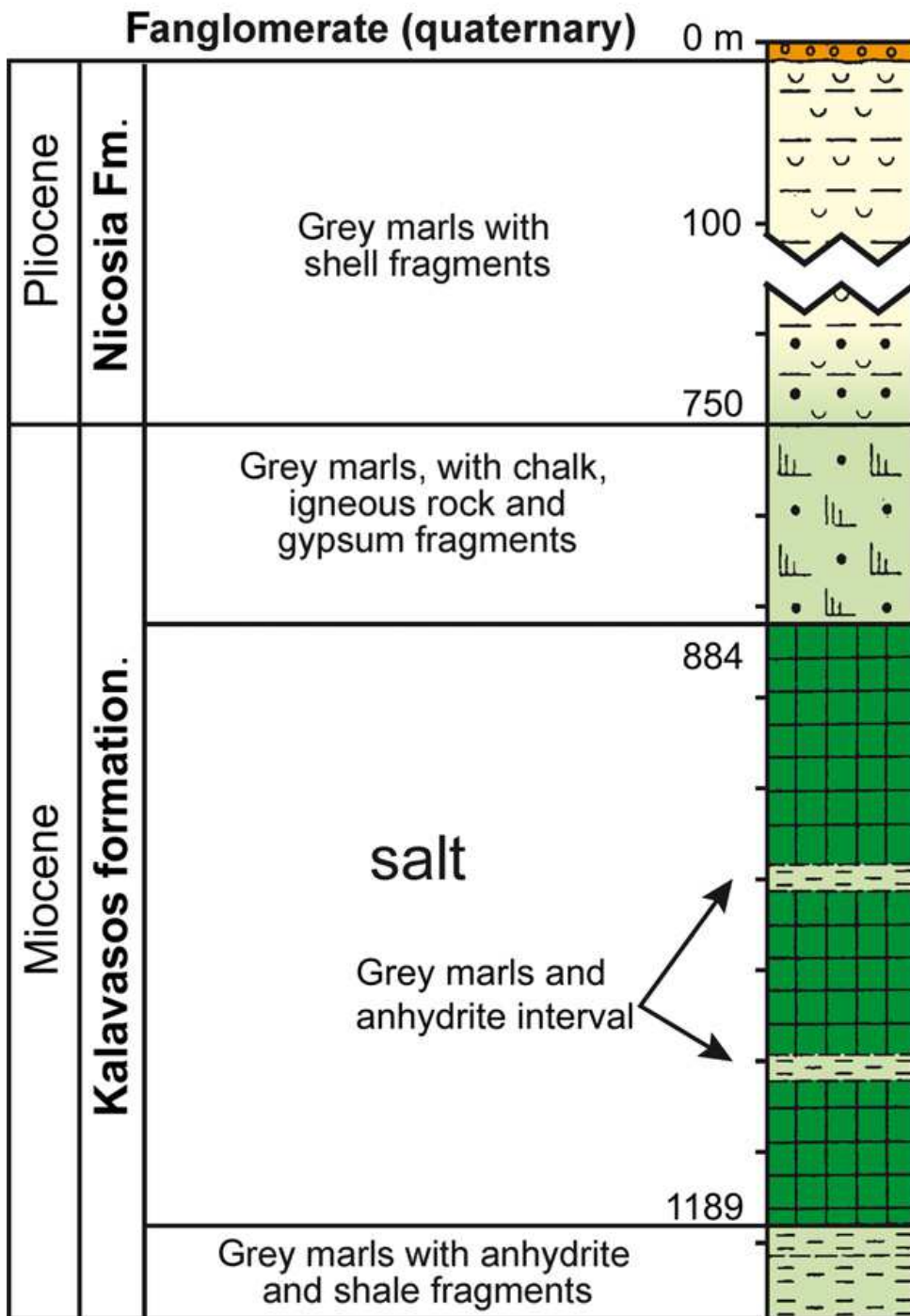
Fig. 15
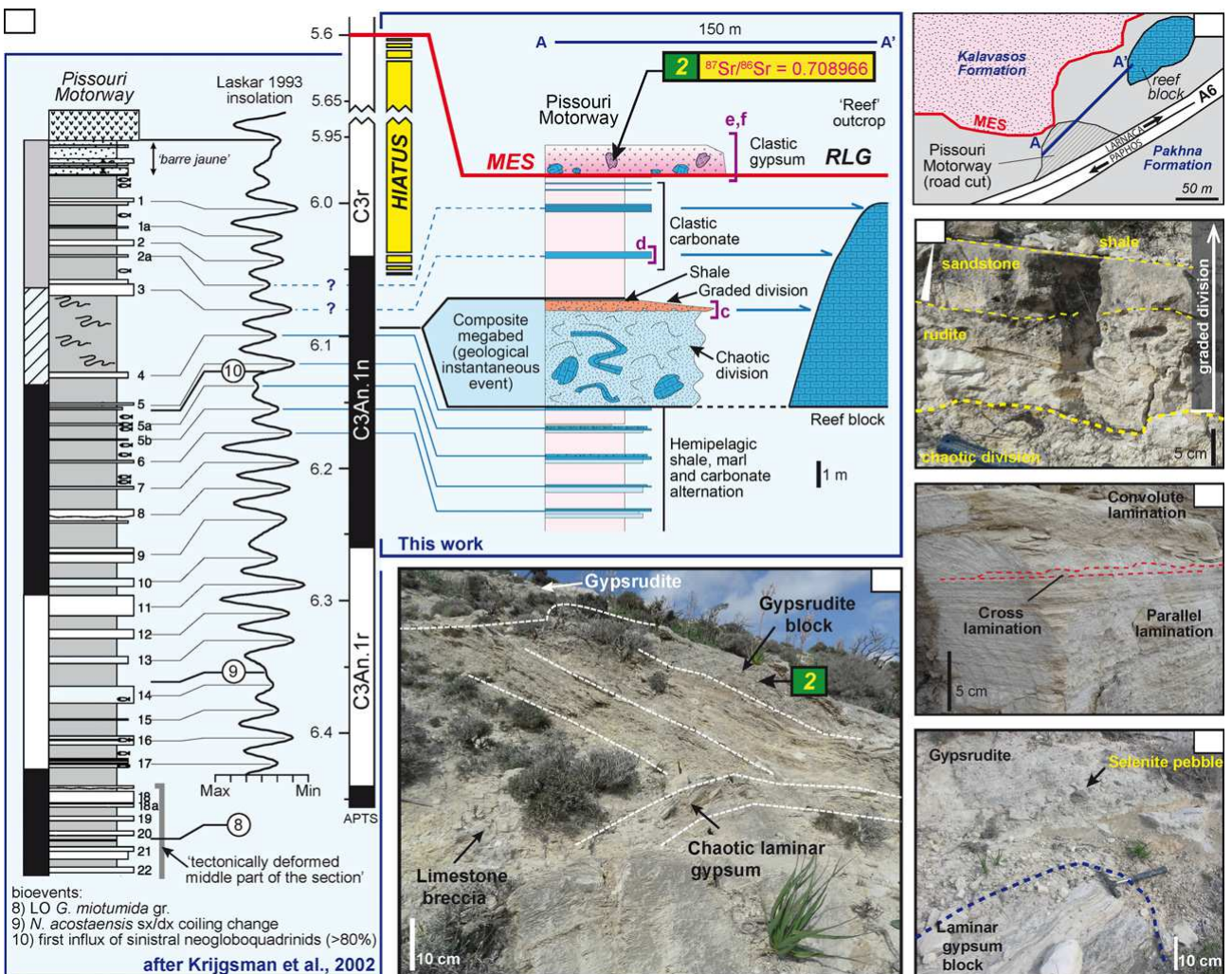
Fig. 16
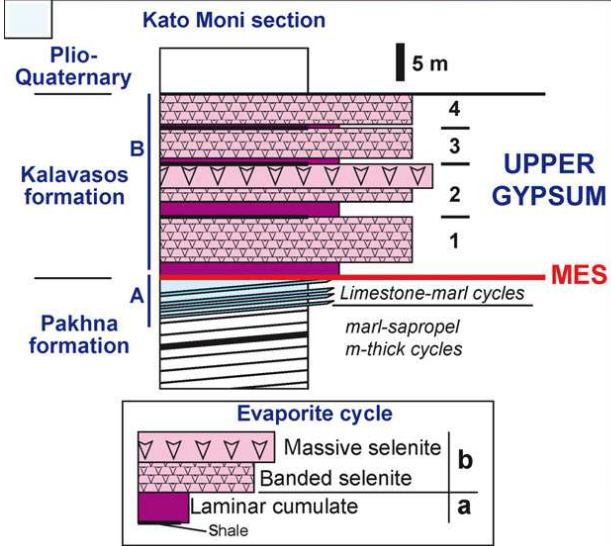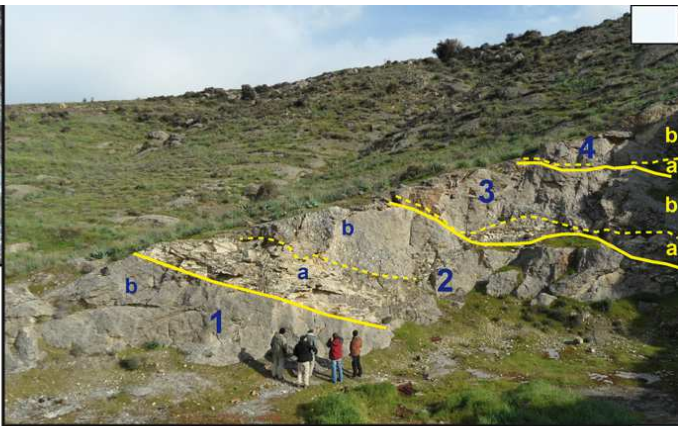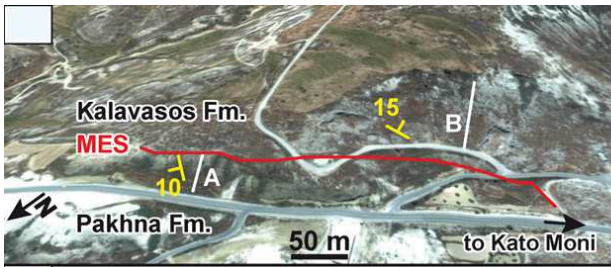
Fig. 17

Xeri borehole (cyprus)
(Gass, 1960)

Fanglomerate (quaternary) — 0 m

Pliocene / Nicosia Fm.

Grey marls with shell fragments — 100

— 750

Grey marls, with chalk, igneous rock and gypsum fragments

884

Miocene / Kalavasos formation.

salt

Grey marls and anhydrite interval

1189

Grey marls with anhydrite and shale fragments

Fig. 18

Fig. 19

Fig. 20

Fig. 21